

Effective Hamiltonians and Phase Diagrams for Tight-Binding Models

Nilanjana Datta,¹ Roberto Fernández,² and Jürg Fröhlich³

Received August 28, 1998; final March 29, 1999

We present rigorous results for several variants of the Hubbard model in the strong-coupling regime. We establish a mathematically controlled perturbation expansion which shows how previously proposed effective interactions are, in fact, leading-order terms of well-defined (volume-independent) unitarily equivalent interactions. In addition, in the very asymmetric (Falicov–Kimball) regime, we are able to apply recently developed phase-diagram technology (quantum Pirogov–Sinai theory) to conclude that the zero-temperature phase diagrams obtained for the leading classical part remain valid, except for thin excluded regions and small deformations, for the full-fledged quantum interaction at zero or low temperature. Moreover, the phase diagram is stable against addition of arbitrary, but sufficiently small further quantum terms that do not break the ground-state symmetries. This generalizes and unifies a number of previous results on the subject; in particular, published results on the zero-temperature phase diagram of the Falicov–Kimball model (with and without magnetic flux) are extended to small temperatures and/or small ionic hopping. We give explicit expressions for the first few orders, in the hopping amplitude, of equivalent interactions, and we describe the resulting phase diagram. Our approach yields algorithms to compute equivalent interactions to arbitrarily high order in the hopping amplitude.

KEY WORDS: Tight-binding models; one-band Hubbard models; three-band Hubbard models; perturbation expansions; phase diagrams; Pirogov–Sinai theory.

¹ Institut de Physique Théorique, EPFL, CH-1015 Ecublens, Lausanne, Switzerland; e-mail: datta@dpmail.epfl.ch.

² Instituto de Estudos Avançados, Universidade de São Paulo, 05508-900 São Paulo, Brazil; e-mail: rf@ime.usp.br.

³ Institut für Theoretische Physik, ETH-Hönggerberg, CH-8093 Zürich, Switzerland; e-mail: juerg@itp.phys.ethz.ch.

1. INTRODUCTION

1.1. Scope of the Paper

In this paper we present rigorous results for several variants of the Hubbard model in the strong-coupling regime. For a general class of Hubbard-type models, we construct effective Hamiltonians with explicit exchange interaction terms by using unitary conjugations obtained from convergent perturbation expansions. Furthermore, we determine ground states and low-temperature phases in the asymmetric (Falicov–Kimball) regime. Our results are applications of tools recently developed in refs. 11 and 12 for the rigorous study of quantum statistical mechanical lattice systems. These tools can be applied to systems with finite-volume Hamiltonians of the form $H_A = H_{0A} + V_A$, where: (1) the dominant part, H_{0A} , is “classical”—in the sense of being diagonal in a tensor-product basis (see Section 2.2 below)—and has a known energy spectrum with spectral gaps uniformly positive in the volume $A \subset \mathbb{Z}^v$, and (2) the perturbation, V_A , must be small in a sense to be made precise below, but can be rather general. In particular, it may involve interactions of infinite range as long as some exponential-decay condition [(2.20) below] is satisfied. For the (one-band) Hubbard-type models to be studied in this paper, H_{0A} involves only on-site terms and the perturbation is just nearest-neighbor hopping. These models rank among the simplest applications of our conjugation method. To illustrate a slightly more complicated application, we also analyze the 3-band Hubbard model.

The methodology used in this paper has two parts: (I) a *rigorously controlled perturbation expansion*, the “conjugation method,” designed to approximately block-diagonalize the Hamiltonians of quantum lattice systems in a spectral range corresponding to low energies, and (II) a theory of stability of phases and phase diagrams known as *quantum Pirogov–Sinai theory*. Part (I) yields a perturbative expansion with mathematically controlled error terms, which agrees, to leading orders, with well known expansions.^(8, 26, 33, 45, 9, 10, 19, 37) Part (II) allows us to extend—and rederive in a more systematic fashion—rigorous results on low-temperature phase diagrams for models such as the Falicov–Kimball model.^(32, 20, 21, 36, 31, 38, 23) Part (I) of our method has a precursor in the method of dressing transformations; (see refs. 15 and 17). Dressing transformations have been used successfully in the study of quantum lattice systems by Albanese.^(1–3)

In the statistical mechanics of classical lattice systems, there exist efficient methods and well tested intuitions to determine and describe ground states and equilibrium states. The mathematical study of quantum lattice systems is less advanced. The loss of the probabilistic framework

—noncommuting observables, complex-valued expectations—necessarily makes an analysis more abstract, and often there is a divorce between the simple and concrete intuitions practitioners resort to and a mathematical approach suitable for rigorous proofs.

The study of quantum perturbations of classical systems offers an excellent opportunity to establish a bridge between the classical and quantum formalisms and to extend techniques and intuitions from the classical realm to the quantum realm in a mathematically controlled manner. This is, in essence, what our methods accomplish.

Of course, the scope of such methods is limited. They are inadequate to rigorously study strong *quantum-mechanical* correlations, such as those appearing in Fermi liquids or superconductors, or to analyze the spontaneous breaking of continuous symmetries. To be more specific, our perturbation expansions and quantum Pirogov Sinai theory converge only if the quantum perturbation V_A is small, in a sense explained later in this paper, as compared to the classical Hamiltonian H_{0A} . But the perturbation expansion enables us to decompose the Hamiltonian H_A into an *effective* classical Hamiltonian and a quantum perturbation in a way that takes into account how the original perturbation V_A lifts degeneracies in the energy spectrum of the original classical Hamiltonian H_{0A} . In particular, it enables us to show how—as a consequence of the Pauli principle—*effective exchange interactions* are generated, starting from a Hamiltonian with *spin-independent* interactions, such as the Hubbard Hamiltonian. The key idea underlying our perturbation technique is to perturbatively construct a *unitary conjugation* of the original Hamiltonian which block-diagonalizes it up to some finite order in the quantum perturbation. It is analogous to Nekhoroshev's method in classical mechanics. The goal of the method is to unitarily conjugate the original Hamiltonian to an effective Hamiltonian of a form that enables us to apply quantum Pirogov–Sinai theory. As a result, we are able to study genuine quantum effects.

The main purpose of this paper is to illustrate the perturbation technique (I) and quantum Pirogov Sinai theory (II) by analyzing concrete models, such as Hubbard-type models, of interest in condensed matter physics. Further applications can be found in refs. 12 and 16.

We emphasize that the two methods, (I) and (II) above, used in this paper are independent of each other. The perturbation method can be applied whenever the leading classical Hamiltonian has an appropriate, essentially volume-independent discrete low-energy spectrum and its ground states simultaneously minimize all local contributions to the classical Hamiltonian (technically, the classical Hamiltonian is assumed to be defined by a so-called m -potentials⁽²⁷⁾—see Section 2), and the quantum perturbation is “small” (see Section 2). It may or may not happen that the

transformed Hamiltonian, the “effective” Hamiltonian, is in a form suitable for the application of quantum Pirogov Sinai theory. If it is, then we are able to rigorously investigate the low-temperature phase diagram in certain regions of the space of thermodynamic parameters. But even if it is not in a form enabling us to apply method (II), it may nevertheless yield new insight into the structure of ground states or low-temperature equilibrium states (by enabling us to e.g., appeal to “educated guesses”). As mentioned, the effective Hamiltonian may, for example, include exchange interactions between spins—absent in the original Hamiltonian—that enable one to determine, at least heuristically, the type of magnetic ordering of the ground states. We are confident that our perturbation method will be useful in providing suitable effective Hamiltonians as starting points for alternative approaches to the study of phase diagrams, such as renormalization group methods.

Recently, an alternative, but related, approach has been put forward in ref. 35 for the analysis of quantum degeneracy-breaking effects. This approach, based on a contour representation very similar to ours,⁽⁵⁾ resorts to a resummation of contours representing low-level excitations to obtain a *classical* effective potential created by the quantum perturbation. In this approach, the perturbative and the contour expansions are closely entangled: the method only works if the resulting effective potential satisfies the hypotheses required by quantum Pirogov–Sinai theory. It is not designed to systematically generate effective Hamiltonians, as in Tables 1 and 2 below. But this alternative approach is a useful first step towards a quantum extension of the theory of *restricted ensembles*.^(6, 44)

A number of delicate concepts are involved when designing mathematically controlled approaches. Some of them are discussed below (Sections 2.1 and 4.1). We would like to start here with a general remark related to the infinite-volume limit: As we are after statistical mechanical properties (phases, phase transitions), we have to pass, eventually, to the thermodynamic limit. This implies that we need to cope with Hamiltonians for arbitrarily large volumes A , e.g., arbitrarily large squares. To achieve this, we shall adopt the following two “principles:”

(P1) We shall attempt to establish estimates or bounds that hold *uniformly* for sufficiently large volumes.

(P2) Instead of working at the level of Hamiltonians, we shall work with so-called *interactions*, which are families of *local* operators $\{\Phi_X: X \subset \mathbb{Z}^v \text{ finite}\}$ (so-called $|X|$ -body terms), in terms of which the Hamiltonians are given by $H_A = \sum_{X \cap A \neq \emptyset} \Phi_X$. Interactions are defined *without* reference to the total volume of the system. Hence operations performed on interactions automatically apply to all finite-volume Hamiltonians.

Next, we proceed to introducing some of the models studied in this paper and to summarizing our main results.

1.2. Models and results

1.2.1. One-Band Hubbard Model. We shall study the one-band Hubbard model and some of its variants. These are models of two types of fermions—which, for concreteness, will be called spin-up and spin-down electrons, but which can also be considered to be different species of particles, like ions and spin-polarized electrons—whose quantum dynamics, on a finite square lattice A , is governed by the Hamiltonian

$$H_A = U \sum_{x \in A} n_{x+} n_{x-} - \mu_+ \sum_{x \in A} n_{x+} - \mu_- \sum_{x \in A} n_{x-} - \sum_{\langle xy \rangle} \sum_{\sigma = +, -} [t_{\sigma}^{[xy]} c_{x\sigma}^{\dagger} c_{y\sigma} + t_{\sigma}^{[yx]} c_{y\sigma}^{\dagger} c_{x\sigma}] \quad (1.1)$$

Here $c_{x\sigma}^{\dagger}$ and $c_{x\sigma}$ are electron creation- and annihilation operators satisfying the usual anticommutation relations [see (2.9)–(2.10)]. The number operator of an electron of spin $\sigma = +, -$ at the site x is $n_{x\sigma} = c_{x\sigma}^{\dagger} c_{x\sigma}$. The chemical potentials of the electrons with up-spin and down-spin are denoted by μ_+ and μ_- , respectively. The symbol $\langle xy \rangle$ (resp. $[xy]$) denotes an unordered (resp. ordered) pair of nearest neighbor sites of the lattice.

The Hubbard model is the simplest model believed to embody the essential physics governing strongly correlated electron liquids. It exhibits the interplay between Coulomb repulsion and the kinetic energy term of electrons. The model is widely studied in the context of phenomena such as magnetism and high- T_c superconductivity, which are believed to result from such an interplay. It is a lattice model of interacting fermions in the tight-binding approximation. The model retains only that part of the (screened) Coulomb repulsion which manifests itself when two electrons of opposite spin occupy the same lattice site, the strength of this interaction being given by the coupling constant U . The kinetic energy term describes the hopping of electrons between nearest-neighbor sites. We allow a direction-dependent hopping: the hopping amplitude of electrons of spin σ from a site x to a site y is denoted by the symbol $t_{\sigma}^{[yx]}$. For the Hamiltonian to be self-adjoint, $t_{\sigma}^{[yx]}$ must be the complex-conjugate of $t_{\sigma}^{[xy]}$. Complex hopping amplitudes are encountered in the presence of an external magnetic field.

If $t_{+}^{[yx]} = t_{-}^{[yx]}$ the Hamiltonian (1.1) does not change under a rotation of the spin quantization axis. Hence the model has an $SU(2)$ symmetry.

This is the case for the standard one band Hubbard model for which $t_+^{[yx]} = t_-^{[xy]} = t$, for all nearest neighbor sites x, y . The highly asymmetric regime $|t_+^{[yx]}| \ll |t_-^{[yx]}|$ will be called the *Falicov–Kimball regime*. The limiting case $t_+^{[yx]} = 0$ constitutes the Falicov–Kimball model (with magnetic flux⁽²³⁾). In this setting, up-spin electrons are interpreted as *static ions*, while down-spin electrons are viewed as scalar quantum-mechanical particles. If the magnetic flux is zero, $t_-^{[yx]}$ is real and independent of x, y .

We study the model (1.1) in the strong coupling limit $U \gg |t_-^{[yx]}|$. This corresponds to the situation in which the Coulomb repulsion is much larger than the bandwidth of (uncorrelated) electrons. The large on-site repulsion forbids double occupancy of a site at zero temperature. In this limit, the terms in the first line on the RHS of (1.1) act as a leading classical part, $H_{0,A}$, while the hopping term can be treated as a perturbation, V_A . As we shall see, this gives rise to a relatively simple application of our perturbation scheme, due to the on-site character of the leading interaction.

To discuss our results, we first present the zero-temperature phase diagram of the dominant part, $H_{0,A}$, of the Hamiltonian, in the plane of the chemical potentials. This is a purely classical interaction, and ground states are tensor products of single-site spin states minimizing each on-site term. It is given in Fig. 1. The symbols $\{+\}$, $\{-\}$, $\{\pm\}$ and $\{0\}$ are used to denote ground states of $H_{0,A}$ in which each lattice site is occupied by an up-spin electron, a down-spin electron, two electrons of opposite spins and no electron, respectively. All the boundary lines in this phase diagram are

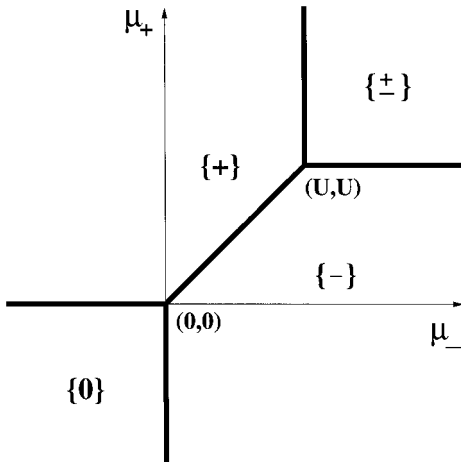


Fig. 1. Zero-temperature phase diagram for $H_{0,A} = U \sum_{x \in A} n_{x+} n_{x-} - \mu_+ \sum_{x \in A} n_{x+} - \mu_- \sum_{x \in A} n_{x-}$. Ground states are defined by spin configurations, which at each site are as denoted in curly brackets.

lines of infinite degeneracy; e.g., for $0 < \mu_+ = \mu_- < U$ the ground state is infinitely degenerate, because all singly occupied configurations are equally likely. The point $\mu_+ = \mu_- = 0$ (origin) and the point $\mu_+ = \mu_- = U$ also correspond to infinitely many ground states. At the origin, each site is either empty or singly occupied, whereas, at the point (U, U) , each site is either singly or doubly occupied. Next, we describe our results for the Hubbard model.

(1) *Controlled Perturbation Expansion.* We restrict our attention to those values of the chemical potentials for which the spectrum of the Hamiltonian $H_{0,A}$ can be decomposed into two spectral bands separated by an energy gap which is large compared to the hopping amplitudes. We discuss mainly the half-filled regime (Section 3), for which the lower band corresponds to the subspace of states with singly occupied sites. In this regime, to have a large-enough spectral gap, we must consider a region in the positive quadrant in the plane of chemical potentials in which $\mu_0 < \mu_+$, $\mu_- < U - \mu_0$, where $\mu_0 \gg |t_{\sigma}^{[yx]}|$. This is the shaded region in the plane of chemical potentials shown in Fig. 2.

For values of the chemical potentials in this shaded region, we determine, for each finite order n , an interaction $\{\Phi_X^{(n)}\}$ that is

(R1) *equivalent* to the one corresponding to (1.1), i.e., it gives rise to Hamiltonians related to (1.1) by a unitary transformation, and

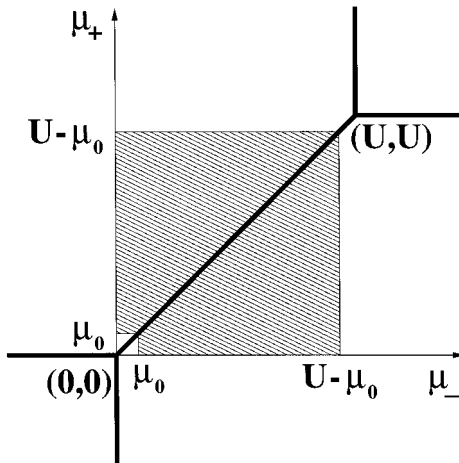


Fig. 2. Shaded region to which we restrict most of the analysis of the generalized Hubbard model (1.1).

(R2) *block-diagonal* to order t^n/U^{n-1} , where $t = \sup_{x,y} \{|t_{-}^{[yx]}|, |t_{+}^{[yx]}|\}$, in the sense that the matrix elements of the operators $\Phi_X^{(n)}$ between the lower and higher bands (of H_{0A}) are of the prescribed order.

Transformations of this sort have been devised before, see for instance refs. 8, 26, 33, 45, 9, 10, 19, and 37, though not in a manner suited for rigorous analysis, as we comment upon below, in Section 2.1. Our expressions, obtained with the technique developed in ref. 12, yield, when restricted to the lower band, the well known leading order terms: Heisenberg interaction + terms of order t^4/U^3 favoring valence-bond states (and breaking the degeneracy among those) + terms of order $t^6/U^5 + \dots$. In particular, they coincide exactly with those of ref. 37, in the half-filled regime. (Our approach can be viewed as a mathematical justification of the series proposed there.) Nevertheless, each transformed interaction $\{\Phi_X^{(n)}\}$ has terms, $\Phi_X^{(n)} \neq 0$, with arbitrarily large $|X|$ but correspondingly small order in t/U , which have been largely ignored in the literature. They are, however, crucial if one wants to determine whether $\{\Phi_X^{(n)}\}$ is indeed an honest interaction or only some auxiliary object corresponding to the first few terms in an asymptotic series. Our approach is designed to settle such issues. In fact, it yields complete mathematical control over the transformed interactions (and the unitary transformations giving rise to them):

(a) We obtain explicit bounds for the error terms, and show that each transformed interaction $\{\Phi_X^{(n)}\}$ is well defined in the strong-coupling regime. (In fact, it is exponentially summable.) We provide explicit estimations of the radius of convergence, $t_0(n)$, and of the exponential decay of the terms $\Phi_X^{(n)}$ in the diameter of X .

(b) We provide explicit algorithms to construct the full interaction $\{\Phi_X^{(n)}\}$, not only its first few orders (restricted to the lowest band).

As we work in terms of interactions, all the expressions, bounds and estimations are, of course, independent of the volume. For the Falicov–Kimball regime, our analysis implies the various estimations obtained, by more cumbersome means, in previous studies of the model^(32, 20, 21, 36, 31, 38, 23) (see also the review in ref. 22).

Similar calculations, that we leave to the reader, can be done in the region of the plane of chemical potentials close to the origin. The low-lying band is now formed by states with no doubly occupied sites. This yields a family of transformed interactions $\{\tilde{\Phi}_X^{(n)}\}$ whose restrictions to the lower band yield the well known perturbation series often associated with the keyword “Gutzwiller projections.” In fact, these series, which start with the very popular $t - J$ interaction plus (usually neglected) three-site terms, are the ones usually reported in the physics literature (see, e.g., refs. 26, 9, 10,

and 37). The half-filled case discussed above is obtained after a further projection onto the half-filled band. Our formalism has, in relation to previous publications, the advantages (a) and (b) described above.

(II) *Phase Diagram at Low Temperatures.* We are able to infer low-temperature properties of the model (1.1), in the strong coupling regime, in the shaded region of Fig. 3, namely away from the manifolds of coexistence of ground states, and at and near the segment along the line $\mu_+ = \mu_-$, as long as we stay clear of its infinitely degenerate endpoints. As we work with contour arguments, we restrict our attention to dimensions $d \geq 2$ and hopping amplitudes $t_\sigma^{[yx]}$ that are *periodic* with respect to translations of the sites x, y . Of course, rigorous control of the ground states and low-temperature equilibrium states *on the “unperturbed” coexistence line* $\mu_+ = \mu_-$ with the help of contour expansions will be achieved only for the models *without* continuous $SU(2)$ -symmetry. We shall prove the following results:

(R3) Inside the (open) regions where H_{0A} has a unique ground state, we apply the cluster expansion developed in ref. 11, Section 6, to conclude that the ground state is stable for small hopping amplitudes and at low temperatures. That is, in these ranges, one finds an equilibrium state for which the observables have expectations close to their values for the corresponding ground state. Such a state can be constructed as the limit of a sequence of states associated with finite boxes with a ground state configuration as boundary condition, and the cluster expansion allows for a visualization (in a very precise sense) of the state as “ground state + quantum and thermal fluctuations.”

(R4) For the Falicov–Kimball regime, $|t_+^{[yx]}| \ll |t_-^{[yx]}|$, we can apply the Pirogov Sinai approach developed in refs. 11 and 12 in conjunction with the transformed interactions $\{\Phi_X^{(n)}\}$ described above, to analyze the shaded region of Fig. 3 at or close to the line $\mu_+ = \mu_-$, for strong Coulomb coupling U . In this way we recover and extend a number of previously published results, prove some expected features of the low-temperature phase diagram and open the way for further systematic analysis of the latter.

In more detail, the results alluded to in (R4) are as follows.

Falicov–Kimball Model Without Flux ($t_-^{[yx]} = t$ for all x, y): (R4.1) As soon as $t \neq 0$, the quantum hopping breaks the infinite-degeneracy present on the line $0 < \mu_+ = \mu_- < U$. Instead two Néel-ordered ground states appear on this line, and in its neighborhood, and remain stable for low temperatures. For the Falicov–Kimball model itself (i.e., when $t_+^{[yx]}$ is

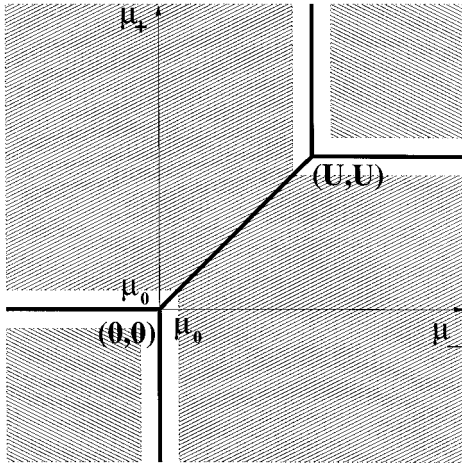


Fig. 3. Region (shown shaded) where low-temperature properties of the model (1.1) are determined in the strong-coupling regime.

exactly zero), this fact has been proven in ref. 32 for chemical potentials on the line itself, and in ref. 36 for potentials in its vicinity. Our methods show that the same is true even if one adds some small ionic hopping (a fact that also follows from the treatment in ref. 38) or, indeed, any other translation-invariant quantum perturbation, which could be long-range but must decay exponentially; see (2.20). Similar results were obtained in ref. 35. (But the authors study only the line $\mu_+ = \mu_-$.)

(R4.2) By considering the transformed interaction, $\{\Phi_X^{(2)}\}$, we can actually show that, for low temperatures and t/U small, a phase diagram as in Fig. 4 appears for the Falicov–Kimball model: There are two “strips” of width of order t^4/U^3 , located around the lines $\mu_+ - \mu_- = \pm 4t^2/U$ for zero temperature, and some smooth deformation [Section 3.2.1] of them for small nonzero temperatures, where nothing can be said. Between them, the states are Néel ordered, while towards the upper left the state is (a thermal perturbation of the ground state) all-“+,” and to the bottom right it is all-“−.” Such a phase diagram has already been established at zero temperature,^(20, 31) but the proof of its stability for small temperatures had to wait until the development of the methods discussed in this paper and the related methods of ref. 35.

(R4.3) Resorting to the next order in the transformation of interactions, i.e., to $\{\Phi_X^{(4)}\}$, we can see in more detail what goes on inside the two excluded regions discussed above. For $d=2$, each region splits into four “strips,” now of width of order t^6/U^5 , that require further investigation

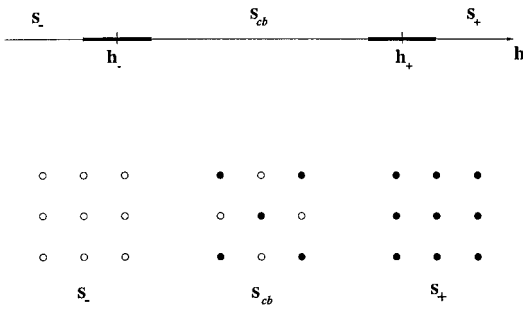


Fig. 4. Phase diagram at zero and low temperatures of the Falicov–Kimball model to order t^2/U , as a function of $h = \mu_+ - \mu_-$. The labels S_+ , S_- and S_{cb} refer to states that are quantum and thermal fluctuations of the indicated configurations or its translations (open circles correspond to “+” particles and closed circles to “-” particles). Thick lines represent excluded regions of width $O(t^4/U^3)$ located around $h_{\pm} = \pm 4t^2/U + O(\varepsilon_{\beta t})$. The small correction $\varepsilon_{\beta t}$ is discussed in Sections 4.4 and 4.5 below.

(Fig. 5), and, between them, a finite number of states appear, which are quantum and thermal perturbations of certain configurations with different proportions of “+” and “-” particles. At zero temperature, these features have been formally calculated in ref. 21 and rigorously established in refs. 31 and 23, and, by a cluster-expansion method, in ref. 38. Our formalism shows that they are also present at small nonzero temperature, except that the excluded manifolds suffer a smooth (and small) deformation.

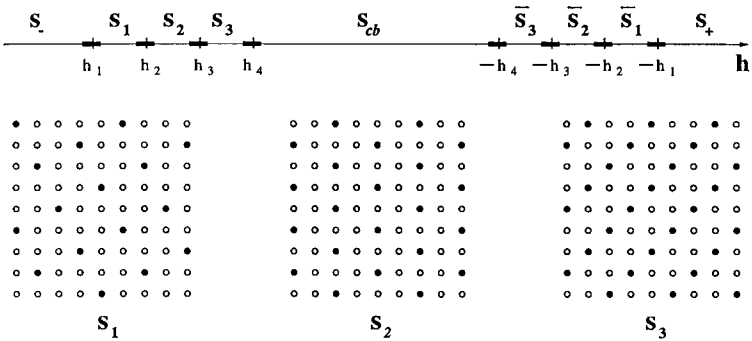


Fig. 5. Phase diagram at zero and low temperatures of the Falicov–Kimball model to order t^4/U^3 , as a function of $h = \mu_+ - \mu_-$. Besides the states of Fig. 4, there appear those corresponding to quantum and thermal fluctuations of rotations and translations of the configurations S_i (depicted) and \bar{S}_i (obtained from the S_i by a $\bullet \leftrightarrow \circ$ interchange). The excluded regions (thick lines) have width $O(t^6/U^5)$ and their location are determined by the values $h_1 = -4t^2/U - 4t^4/U^3 + O(\varepsilon_{\beta t})$, $h_2 = -4t^2/U + 16t^4/U^3 + O(\varepsilon_{\beta t})$, $h_3 = -4t^2/U + 48t^4/U^3 + O(\varepsilon_{\beta t})$ and $h_4 = -4t^2/U + 84t^4/U^3 + O(\varepsilon_{\beta t})$.

(R4.4) At the next order, t^6/U^5 , each of the eight precedent strips is expected to open up into eight finer strips outside of which there is only a finite ground state degeneracy. Our formalism would then yield stability of this structure when the temperature is increased or further small quantum perturbations are added. In fact, a “devil’s staircase” is expected to appear in this way, to successively larger orders t^n/U^{n-1} .^(25,47) While we do not work out any details we think that this paper provides enough tools for a motivated reader to pursue these issues: It provides algorithms for the higher-order transformed interactions $\{\Phi_X^{(n)}\}$, the certainty that the remainders are rigorously controlled to the specified order, and conditions to predict stability. Of course, in order to get precise results, one has to come up with an accurate determination of the ground states of the classical leading part of the transformed interactions. This tends to be the hardest part of the work. The beautiful method introduced in ref. 31 (see also the application in [ref. 23, Appendix A]) could be very helpful at this point.

An advantage of our methods is their robustness with respect to perturbations: All the results sketched above remain valid if we add an arbitrary, but small enough, quantum perturbation that respects the symmetries connecting the different ground states (typically invariant under translations and 90° -rotations). In particular, they extend to the Falicov–Kimball *regime* (i.e., $|t_+^{[yx]}|$ small, but not necessarily zero), and to models including additional perturbations, which can possibly be long-range but must decay exponentially; see (2.20).

Our methods are not suited for the study of the phase diagram of the $SU(2)$ -symmetric Hubbard model, because continuous symmetry breaking is accompanied by the appearance of gapless modes. In particular, we cannot apply our phase-diagram technology to the effective Hamiltonians that would be obtained via Gutzwiller projections ($t - J$ interaction + higher orders). But we emphasize that the perturbation technique (I) is applicable in such situations.

Falicov–Kimball Model with Flux [$t_-^{[yx]} = t \exp(i\theta_{yx})$], with $\theta_{yx} \in [0, 2\pi]$. The previous results can be extended to the model with flux, starting from the study of ground states presented in ref. 23. For this case, the results (R4.1) and (R4.2) remain valid, because the properties involved are independent of the flux. Regarding (R4.3), the positions of the excluded regions do depend on the flux, but the ground states around them do not (see Section 3.2.1 in ref. 23). Our methods show that these ground states remain stable at small temperature and/or under the addition of small translation- and rotation-invariant quantum perturbations (e.g., ionic motion).

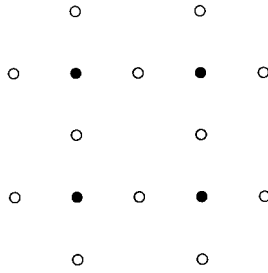


Fig. 6. Lattice for the 3-band Hubbard model. The open circles denote oxygen sites while the closed circles denote copper sites.

1.2.2. 3-Band Hubbard Model. As an illustration of the use of our perturbation technique for models whose leading interaction is not strictly on-site, we consider the 3-band Hubbard model, which was first introduced by Emery to describe the behaviour of the charge carriers in the CuO_2 planes of cuprates exhibiting high- T_c superconductivity. The model is defined on a two-dimensional lattice, a unit cell of which contains one copper and two oxygen atoms (Fig. 6).

The copper atoms form a square lattice, and there is an oxygen atom between each nearest neighbor copper-copper pair.

The charge carriers are spin-1/2 holes which can hop between the d -orbital of a copper atom and the p -orbital of an adjacent oxygen atom. We shall refer to this as the hopping of holes between a copper site and an oxygen site. The Hamiltonian governing the model defined on a finite lattice $A := A \cup B$, where A denotes the sublattice of copper atoms and B denotes the sublattice of oxygen atoms, is given as follows:

$$\begin{aligned}
 H_A = & \left\{ U_d \sum_{x \in A} n_{x+}^d n_{x-}^d + U_p \sum_{y \in B} n_{y+}^p n_{y-}^p + U_{pd} \sum_{\langle xy \rangle} n_x^d n_y^p \right. \\
 & \left. + \varepsilon_d \sum_{x \in A} n_x^d + \varepsilon_p \sum_{y \in B} n_y^p \right\} + \left\{ t_{pd} \sum_{\langle xy \rangle} \sum_{\sigma = +, -} [p_{y\sigma}^\dagger d_{x\sigma} + d_{x\sigma}^\dagger p_{y\sigma}] \right\} \\
 := & H_{0A} + V_A(t_{pd})
 \end{aligned} \tag{1.2}$$

The number operator for a hole at the site $x \in A$ is $n_x^d = (n_{x+}^d + n_{x-}^d)$, where $n_{x\sigma}^d = d_{x\sigma}^\dagger d_{x\sigma}$, for $\sigma \in \{+, -\}$, with $d_{x\sigma}^\dagger$ and $d_{x\sigma}$ denoting fermion creation- and annihilation operators for a hole of spin σ at the site x . The corresponding number operator for a hole at the site $y \in B$ is $n_y^p = (n_{y+}^p + n_{y-}^p)$ where $n_{y\sigma}^p = p_{y\sigma}^\dagger p_{y\sigma}$, with $p_{y\sigma}^\dagger$ and $p_{y\sigma}$ the fermion creation- and annihilation

operators for a hole of spin σ in the p -orbital of an oxygen atom. The coefficients U_d and U_p denote the strengths of the on-site repulsions between two holes of opposite spin when they occupy a copper site and an oxygen site, respectively. In addition to this on-site interaction, two holes experience a Coulomb repulsion of strength U_{pd} when they occupy adjacent copper and oxygen sites. The on-site energies for the copper and the oxygen are denoted by the symbols ε_d and ε_p , respectively, and the charge transfer gap is given by

$$\Delta := \varepsilon_p - \varepsilon_d \quad (1.3)$$

The hopping amplitude of a hole between a copper site and an oxygen site is denoted by t_{pd} and is proportional to an overlap integral of atomic orbitals. Often a small additional term representing the direct hopping of a hole between the p -orbitals of two oxygen atoms is included in the Hamiltonian, but we neglect it here.

Band-structure calculations of cuprates exhibiting high- T_c superconductivity show that it is not unreasonable to study this model assuming

$$\Delta > 0; \quad U_d \gg U_p > U_{pd} > 0; \quad U_d \gg \Delta; \quad t_{pd} > 0 \quad (1.4)$$

and considering the *strong coupling regime* $U_d \gg t_{pd}$. (For instance, in refs. 28 and 29, the estimated values are $\Delta = 3.6$ eV, $U_d = 10.5$ eV, $U_p = 4$ eV, $U_{pd} = 1.2$ eV and $t_{pd} = 1.3$ eV.) We observe that: (i) we can treat $V_A(t_{pd})$ as a perturbation of H_{0A} ; (ii) since $\Delta > 0$, holes prefer to reside on copper sites rather than on oxygen sites, and (iii) since U_d is positive and large, double occupancy of holes at a copper site is energetically unfavorable.

We restrict our attention to the situation in which the total number of holes, N_h , in the lattice A is equal to the total number of copper sites $|A|$:

$$N_h = |A| \quad (1.5)$$

For this choice, a ground-state configuration of H_{0A} has a single hole at each copper site, there being no holes at the oxygen sites. [Equivalently, we could introduce suitable "chemical potentials" and work in the region of parameter space where the ground states have this property.] The hole at a copper site can, however, be either spin-up or spin-down. Hence, the ground state of H_{0A} has a $2^{|A|}$ -fold spin degeneracy.

By resorting to our perturbation expansion, we obtain an equivalent interaction that only involves copper atoms, which includes an antiferromagnetic Heisenberg term. This does not settle the question of whether the hopping term $V_A(t_{pd})$ lifts the spin-degeneracy, because, as mentioned

above, our methods to determine stable phases do not work in the situation where a continuous symmetry [here $SU(2)$] can be broken spontaneously. Nevertheless, our methods show that the transformed interaction is mathematically well defined and provide error estimates which should be valuable in future studies. The form of the transformed interaction is well known. (Indeed, the fact that the leading terms coincide with those of the transformed interaction for the one-band model is an argument favoring the study of the latter rather than of the more cumbersome 3-band model).

It should be noted that the perturbative analysis of models with classical interactions that are not on-site is more difficult, technically, than the one of models with single-site classical interactions, such as the single-band Hubbard model. Our presentations in Sections 2 and 6 will serve to illustrate this point.

2. THE PERTURBATION TECHNIQUE

2.1. Foreword

In quantum mechanics, Rayleigh–Schrödinger perturbation theory can be formulated as the perturbative construction of unitary conjugations transforming a Hamiltonian of the form $H = H_0 + tV$ into a new Hamiltonian, $H' = H'_0(t) + V'(t)$, with the property that $H'_0(t)$ is block-diagonal (in the eigenbasis of H_0), and $V'(t)$ is a perturbation of order t^{m+1} . The operators $H'_0(t)$ and $V'(t)$ are given in terms of power series, and it is important to analyze the convergence properties of these series. Kato's analytic perturbation theory^(30, 42) offers criteria that guarantee convergence: Suppose we attempt to block-diagonalize the Hamiltonian H with respect to a spectral projection of H_0 corresponding to a bounded subset of the spectrum of H_0 separated from its complement by an energy gap $\delta > 0$. Let us assume that the perturbation V is relatively bounded with respect to H_0 , e.g., in the sense that there exist finite (non-negative) constants a and b such that

$$\|V\psi\| \leq a \|H_0\psi\| + b \|\psi\| \quad (2.1)$$

for all vectors ψ in the domain of H_0 . Then perturbation theory for the block-diagonalization of H with respect to the given spectral projection converges, provided

$$|t| a < 1, \quad \frac{|t|}{\delta} (a + b) < C \quad (2.2)$$

where C is a constant that depends on the choice of the spectral projection.

Unfortunately, this result cannot be applied directly to the study of systems of quantum statistical mechanics. The reasons are as follows.

(SM1) First, we do not just want to block-diagonalize a single Hamiltonian H but a *family* of Hamiltonians $\{H_{\mathcal{A}}\}$ indexed by an increasing sequence of finite regions \mathcal{A} of an infinite lattice. In this setting, Kato theory is *not* applicable, because the norms $\|H_{0\mathcal{A}}\|$ and $\|V_{\mathcal{A}}\|$ are typically proportional to the volume $|\mathcal{A}|$, and this usually implies that the constant b in (2.1) is proportional to the volume $|\mathcal{A}|$, too. As a consequence, the radius of convergence of plain Rayleigh–Schrödinger perturbation series tends to zero, as $|\mathcal{A}|$ tends to ∞ . This makes it impossible to establish facts valid in the thermodynamic limit by straightforward use of Rayleigh–Schrödinger–Kato analytic perturbation theory. (Even if $H_{0\mathcal{A}}$ has a *finite* ground state degeneracy, *uniformly* in \mathcal{A} , a naive application of Kato theory does not prove that the perturbation series for the perturbed ground state energy density, for example, converges uniformly in \mathcal{A} .)

(SM2) Second, to study the phase diagram of the system, the transformed Hamiltonians $H'(t)$ must be expressed again in terms of *local* interactions. That is, the unitary conjugations must lead to a block-diagonalization at the level of local *interactions*, rather than just at the level of Hamiltonians. To satisfy this requirement, we find that these conjugations must themselves be defined by (exponentials of) sums of local operators. Furthermore, the original interaction and the local operators defining the conjugation must decrease exponentially in the size of the lattice region in which they are localized.

Keeping in mind these requirements, it is natural to search for transformations whose generators S are sums of local terms, $S = \sum S_Y$, where each S_Y is localized in the region Y , in the sense that it commutes with local operators Φ_X , provided X and Y are disjoint. To achieve this, we incorporate two crucial ingredients in our expansion:

(I1) Defining *local* ground states (of the leading part $H_{0\mathcal{A}}$), we decompose each term Φ_X according to how it acts on states that are local ground states only in the vicinity of X . This is achieved by introducing suitable *local* projectors (P_Y^0 , P_Y^1 and P_Y^2 below).

(I2) We introduce *protection zones* to decouple sufficiently far separated excitations. If we normalize the H_0 -energy of local ground states to be 0 then the H_0 -energy of a configuration of local excitations (local deviations from ground states) separated by protection zones is additive in the H_0 -energies of the excitations.

Ingredient (I2) is irrelevant for the discussion of models, such as the one-band Hubbard model, where the leading interaction is on-site. In such models, the H_0 -energy of excitations localized at different sites is additive. But this is untypical, and in the study of more general models (I2) plays an important role. Regarding ingredient (I1), one finds that it has been used by some authors,^(9, 19, 37, 14) but it has been ignored by others.^(8, 33, 45, 10, 46) The latter use “global” projections involving all sites in a given region A , which lead to volume-dependent expansions with a shrinking convergence radius as mentioned in (SM1). Nevertheless, they appear to obtain correct perturbative results for certain infinite-volume expectation values and for (intensive) thermodynamic quantities, like ground-state energy densities. The problem with their methods is that they do not offer a handle to *proving* (rigorously) that, indeed, their predictions are correct or to determine whether the corresponding series are *convergent* rather than just asymptotic. Expansion schemes such as ours, yielding volume-independent effective interactions, are suitable to answer such mathematical questions. To accomplish this, they must, however, be supplemented with an appropriate construction of ground- and Gibbs states for the transformed Hamiltonian. This is not an easy matter, in general, and it is here that quantum Pirogov–Sinai theory will enter the scene.

We are able to provide a complete picture of the models analyzed in Section 5, below, where Gibbs states are constructed through quantum Pirogov–Sinai theory. In regions of stable phases, the cluster expansion methods we use imply the analyticity of expectations and of thermodynamic potentials as functions of the couplings. For those models, therefore, we are able to prove that the series obtained for expectations of local observables and for intensive quantities are well defined and convergent.

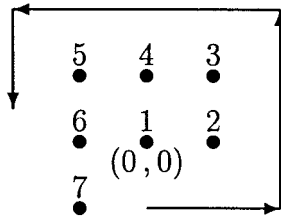
2.2. Notation, Definitions and Preliminary Results

In this section, we review the different elements of our general perturbation technique. (For further details see ref. 12.)

2.2.1. Bases and Operators

The Hilbert Space. We consider a quantum-mechanical system associated with a finite subset A of a ν -dimensional lattice \mathbb{Z}^ν . To each site x in the lattice is associated a Hilbert space \mathcal{H}_x . We require that there be a Hilbert space isomorphism $\varphi_x: \mathcal{H}_x \rightarrow \mathcal{H}$, for all $x \in \mathbb{Z}^\nu$, \mathcal{H} being a fixed, finite-dimensional Hilbert space. The Hilbert space of the region A is given by the ordered tensor product space

$$\mathcal{H}_A = \bigotimes_{x \in A} \mathcal{H}_x \quad (2.3)$$

Fig. 7. Spiral order in \mathbb{Z}^2 .

To avoid ambiguities in the definition of the tensor product (2.3), we choose a total ordering (denoted by the symbol \preceq) of the sites in \mathbb{Z}^v . For convenience we choose an order with the property that, for any finite set X , the set $\bar{X} := \{z \in \mathbb{Z}^v, z \preceq X\}$ of lattice sites which are smaller than X , or belong to X , is finite. For example, for $v=2$ we can use the *spiral order* depicted in Fig. 7.

Tensor Product Basis of \mathcal{H}_A . Let I be an index set and let $\{e_j\}_{j \in I}$ be an orthonormal basis of \mathcal{H} . Then $\{e_j^x\}_{j \in I}$, where $e_j^x = \varphi_x^{-1} e_j$, is an orthonormal basis of \mathcal{H}_x .

A configuration ω on A is an assignment $\{j_x(\omega)\}_{x \in A}$ of an element $j_x \in I$ to each $x \in A$. For $X \subset A$, let ω_X denote the restriction of the configuration ω to the subset X . The set of all configurations in A is denoted by

$$\mathcal{C}_A := \{\omega \mid j_x(\omega) \in I, x \in A\} \quad (2.4)$$

There is a one-to-one correspondence between configurations ω in A and basis vectors

$$e(\omega) := \bigotimes_{x \in A} e_{j_x(\omega)}^x \quad (2.5)$$

of \mathcal{H}_A . A tensor product basis of \mathcal{H}_A is given by $\{e(\omega)\}_{\omega \in \mathcal{C}_A}$.

Local Algebras of Gauge-Invariant Operators. Let $\mathcal{B}(\mathcal{H}_A)$ be the algebra of all bounded operators on \mathcal{H}_A . Let $\{U(\theta) \mid \theta \in \mathbf{R}\}$ be a one-parameter unitary group on \mathcal{H}_A (gauge group of the first kind) with the property that the vectors $e(\omega)$ defined in (2.5) are eigenvectors of $U(\theta)$, for all θ . For any $X \subseteq A$, we define a local algebra $\mathcal{A}_X \subset \mathcal{B}(\mathcal{H}_A)$ of gauge-invariant operators with the following properties:

- If $\{e(\omega)\}_{\omega \in \mathcal{C}_A}$ is an arbitrary tensor product basis of \mathcal{H}_A then

$$\langle e(\omega'), ae(\omega) \rangle = 0 \quad (2.6)$$

unless $\omega'|_{A \setminus X} = \omega|_{A \setminus X}$, for **all** operators $a \in \mathcal{A}_X$. (Here $\langle \psi, \varphi \rangle$ denotes the scalar product of two vectors ψ and φ in \mathcal{H}_A .)

- $U(\theta) a U(\theta)^* = a$, for all $a \in \mathcal{A}_X$, for arbitrary $X \subset A$; (gauge-invariance).
- If $X \subset Y$ then $\mathcal{A}_X \subset \mathcal{A}_Y$.
- If $X \cap Y = \emptyset$ then

$$[a, b] = 0 \quad (2.7)$$

for any $a \in \mathcal{A}_X$ and any $b \in \mathcal{A}_Y$.

Example. Gauge-invariant polynomials in fermion creation- and annihilation operators. Let

$$\{c_{x\sigma}, c_{x\sigma}^\dagger \mid x \in A, \sigma = +, -\} \quad (2.8)$$

denote the usual fermion creation- and annihilation operators satisfying the canonical anti-commutation relations

$$\{c_{x\sigma}, c_{y\sigma'}\} = \{c_{x\sigma}^\dagger, c_{y\sigma'}^\dagger\} = 0 \quad (2.9)$$

and

$$\{c_{x\sigma}, c_{y\sigma'}^\dagger\} = \delta_{xy} \delta_{\sigma\sigma'} \quad (2.10)$$

Of course, σ is the spin index. We define

$$U(\theta) = \exp(i\theta N), \quad \text{where } N = \sum_{\substack{x \in A \\ \sigma \in \{+, -\}}} c_{x\sigma}^\dagger c_{x\sigma} \quad (2.11)$$

The local algebras \mathcal{A}_X , $X \subseteq A$, are defined by

$$\mathcal{A}_X = \{a \mid a \text{ is an arbitrary polynomial in } c_{x\sigma}, c_{x\sigma}^\dagger, x \in X, \sigma \in \{+, -\} \\ \text{with the property that } U(\theta) a U(\theta)^* = a\} \quad (2.12)$$

The Algebra of Local, Gauge-Invariant Operators. Since $\mathcal{A}_X \subset \mathcal{A}_Y$, for $X \subset Y$, we may consider the (inductive) limit $\bigvee_{X \nearrow \mathbb{Z}^v} \mathcal{A}_X$. The algebra \mathcal{A} is defined to be the closure of $\bigvee_{X \nearrow \mathbb{Z}^v} \mathcal{A}_X$ in the operator norm and is called the algebra of all local, gauge-invariant operators.

2.2.2. Interactions and Ground States

Classical Operators and Interactions. An operator a is “classical” w.r.t. a given tensor product basis $\{e(\omega)\}$ if and only if $e(\omega)$ is an eigenvector of a , for all $\omega \in \mathcal{C}_A$. An interaction $\{\Phi_{0X}\}$ is said to be a “classical interaction” (w.r.t. $\{e(\omega)\}_{\omega \in \mathcal{C}_A}$) if and only if the following conditions hold:

1. $\Phi_{0X} \in \mathcal{A}_X$ is a classical operator w.r.t. $\{e(\omega)\}$, for all $X \subseteq A$.
2. More precisely,

$$\Phi_{0X}e(\omega) = \Phi_{0X}(\omega) e(\omega), \quad \Phi_{0X}(\omega) \in \mathbb{R} \quad (2.13)$$

where $\Phi_{0X}(\omega)$ only depends on $\omega|_X$.

[Note that 2 follows from 1 and from (2.7)].

m-Potentials. Let $\Phi_0 = \{\Phi_{0X}\}$ be a classical interaction. We shall always assume that there is at least one configuration, ω_0 , minimizing all Φ_{0X} , i.e.,

$$\Phi_{0X}(\omega_0) = \min_{\omega} \Phi_{0X}(\omega) \quad (2.14)$$

for all X ; (this assumption holds if Φ is given in terms of a so-called *m-potential*⁽²⁷⁾). We normalize the operators Φ_{0X} such that $\Phi_{0X}(\omega_0) = 0$, for all X . Thus

$$\Phi_{0X}(\omega) \geq 0 \quad \text{and} \quad \min_{\omega} \Phi_{0X}(\omega) = 0 \quad (2.15)$$

for all X .

Local Ground States. A configuration ω is said to be a *local ground-state configuration* for a classical interaction Φ_0 and a subset X of the lattice if

$$\Phi_{0Y}(\omega) = 0 \quad \text{for all } Y \subseteq X \quad (2.16)$$

The local Hamiltonians $H_{0X} = \sum_{Y \subseteq X} \Phi_{0Y}$ thus have the property that

$$H_{0X}e(\omega) = 0 \quad (2.17)$$

whenever ω is a local ground state configuration for X . A state e is said to be a *local ground state* for a region X if e is an arbitrary linear combination of the vectors $e(\omega)$, where ω ranges over the local ground state configurations for X .

We shall always assume that the spectrum of H_{0X} has a gap above 0 which is bounded from below by a positive X -independent constant, for all bounded sets X . This assumption can be derived from suitable assumptions on the classical interaction Φ_0 (Φ_0 should be an m -potential with a finite number of periodic ground states, see ref. 27).

The Full Interaction. We consider quantum lattice systems whose dynamics is encoded in an interaction Φ which is assumed to be of the form

$$\Phi = \Phi_0 + Q(\lambda) \quad (2.18)$$

where $\Phi_0 = \{\Phi_{0X}\}$ is a finite-range classical interaction given in terms of an m -potential, and $Q(\lambda) = \{Q_X(\lambda)\}$ is a perturbation interaction with $\lambda = \{\lambda_1, \dots, \lambda_k\}$ a family of real or complex perturbation parameters. For brevity, we shall say that a set X is a *classical bond* if $\Phi_{0X} \neq 0$, and a *quantum bond* if $Q_X(\lambda) \neq 0$. The operators Φ_{0X} and $Q_X(\lambda)$ belong to the local algebra \mathcal{A}_X . A polynomial $p(\lambda)$ is said to be of degree n if

$$p(\lambda) = \sum c_{n_1 \dots n_k} \lambda_1^{n_1} \dots \lambda_k^{n_k} \quad (2.19)$$

with $n = \max\{\sum_{j=1}^k n_j : c_{n_1 \dots n_k} \neq 0\}$. We assume that the leading order in λ of the Interaction $Q(\lambda)$ in (2.18) is of degree 1 (i.e., linear in λ).

We also assume that the interaction $Q(\lambda) = \{Q_X(\lambda)\}$ is either of finite range or decays exponentially in the size of its support, i.e., that there exist an $r > 0$ such that

$$\sum_{X \ni 0} \sqrt{\text{tr}[Q_X^*(\lambda) Q_X(\lambda)]} e^{rs(X)} < \infty \quad (2.20)$$

where $s(X)$ denotes the cardinality of the smallest connected subset of the lattice which contains X . The interaction $Q(\lambda)$ will be treated as a perturbation.

Remark. Roughly speaking, we shall always split the Hamiltonian H_A into a sum of an unperturbed operator H_{0A} and a perturbation $V_A(\lambda)$ in such a way that all low-lying eigenstates of H_A , corresponding to eigenvalues separated from the rest of the spectrum of H_A by a positive (A -independent) gap, correspond to *degenerate ground states* of H_{0A} . More precisely, we choose the classical interaction Φ_0 in such a way that all local low-energy eigenstates of the local Hamiltonians H_{0X} , for $X \subset A$ are *exactly degenerate* in energy; small *degeneracy-lifting* terms are systematically put

into the interaction $Q(\lambda)$ defining the perturbation $V_A(\lambda)$. In a general exposition of our methods, this is a very convenient way of ensuring that H_0 -energies of sufficiently far separated local excitations are *additive*. (Of course, in a concrete model, additivity of H_0 -energies of local excitations may hold for independent reasons; see e.g., Section 3.)

2.2.3. Projection Operators. Protection Zones

“Diagonal” and “Off-Diagonal” Operators. Given a partition of unity

$$\mathbf{1} = \sum_{j=1}^N P_j, \quad P_i P_j = \delta_{ij} P_j, \quad P_i^* = P_i \quad (2.21)$$

and an operator Q , we set

$$Q^{ij} = P_i Q P_j \quad (2.22)$$

We will call the operators Q^{ii} “diagonal,” and the operators Q^{ij} , $i \neq j$, “off-diagonal” (with respect to the given partition of unity).

Protection Zones. To deal properly with the local nature of different operators we define, for any $x \in \mathbb{Z}^v$, a so-called *R-plaquette centered at x*:

$$W_x := \{y \in \mathbb{Z}^v: |y_i - x_i| \leq R, \text{ for } 1 \leq i \leq v\} \quad (2.23)$$

where R is the range of the interaction Φ_0 . For any finite set $X \subset \mathbb{Z}^v$, its covering by R -plaquettes is denoted by

$$B_X := \bigcup_{x \in X} W_x \quad (2.24)$$

The set $B_X \setminus X$ can be interpreted as a *protection zone* around X .

Local Projections. We introduce some special projection operators on the Hilbert space \mathcal{H}_A :

1. If $Y \subset A$ then P_Y^0 is the orthogonal projection onto local ground states for Y . If $Z \subseteq Y$ then $P_Z^0 \supseteq P_Y^0$.

2. The orthogonal projection onto the space of states which are ground states on $B_X \setminus X$, but fail to be ground states on X :

$$P_{B_X}^1 := P_{B_X \setminus X}^0 - P_{B_X}^0 \quad (2.25)$$

Hence $P_{B_X}^1$ projects onto the space of states which have an excitation *localized* in X . The set $B_X \setminus X$ acts as a “protection zone” introduced to ensure the additivity of energies of disconnected excitations [see (2.30) below].

3. The projection onto states with excitations in the “protection zone” $B_X \setminus X$:

$$P_{B_X}^2 := \mathbf{1} - P_{B_X \setminus X}^0 \quad (2.26)$$

where $\mathbf{1}$ is the identity operator.

Additivity of Excitation Energies. For each finite $X \subset \mathbb{Z}^v$, we can decompose the Hamiltonian H_{0A} as follows:

$$H_{0A} = \bar{H}_{0X} + \bar{H}_{0B_X^c} + H_{0B_X \setminus X} \quad (2.27)$$

where $B_X^c = A \setminus B_X$,

$$H_{0A} = \sum_{Y \subset A} \Phi_{0Y} \quad (2.28)$$

and

$$\bar{H}_{0A} = \sum_{Y \cap A \neq \emptyset} \Phi_{0Y} \quad (2.29)$$

If $\psi \in \text{Ran } P_{B_X \setminus X}^0$ then

$$\begin{aligned} H_{0A} \psi &= (\bar{H}_{0X} + H_{0B_X \setminus X} + \bar{H}_{0B_X^c}) \psi \\ &= (\bar{H}_{0X} + \bar{H}_{0B_X^c}) \psi \end{aligned} \quad (2.30)$$

This follows, because $H_{0B_X \setminus X} \psi = H_{0B_X \setminus X} P_{B_X \setminus X}^0 \psi = 0$. Hence, on states ψ corresponding to ground-state configurations in the region $B_X \setminus X$, energies are additive.

2.2.4. Operator Identities

The Lie-Schwinger Series. With this expression we shall refer to the following expansion:

$$\begin{aligned} e^A B e^{-A} &= B + [A, B] + \frac{1}{2!} [A, [A, B]] + \dots \\ &= \sum_{n=0}^{\infty} \frac{1}{n!} \text{ad}^n A(B) \end{aligned} \quad (2.31)$$

Here we use the notation

$$\begin{aligned} \text{ad } A(B) &= [A, B]; \\ \text{ad}^2 A(B) &= [A, [A, B]]; \\ \text{ad}^n A(B) &= [A, \text{ad}^{n-1}(B)] \end{aligned} \quad (2.32)$$

and the convention

$$\text{ad}^0 A(B) = B \quad (2.33)$$

The “ad⁻¹” Operation. Given a self-adjoint operator H whose spectrum consists only of eigenvalues E_i , $i = 1, 2, \dots$, and an operator Q which is purely “off-diagonal” with respect to the partition of unity given by the projections P^i onto the eigenspaces corresponding to each E_i , we define

$$\text{ad}^{-1} H(Q) = \sum_{ij} P^i \frac{Q}{E_i - E_j} P^j \quad (2.34)$$

The right hand side is well defined, because Q is an off-diagonal operator. Of course, ad^{-1} is the operation inverse to ad , i.e.,

$$[H, \text{ad}^{-1} H(Q)] = Q \quad (2.35)$$

2.3. First-Order Perturbation Theory

The first step in our perturbation technique consists in eliminating “off-diagonal” operators of lowest order in λ . Here “off-diagonal” refers to the partitions of unity

$$\mathbf{1} = P_{B_X}^0 + P_{B_X}^1 + P_{B_X}^2 \quad (2.36)$$

In the following, we usually suppress the explicit dependence of the operators $Q_X(\lambda)$ on λ . We rewrite $Q_X \equiv Q_X(\lambda)$ as

$$Q_X = Q_{B_X}^{00} + Q_{B_X}^{01} + Q_{B_X}^R \quad (2.37)$$

where $Q_{B_X}^{00}$ is a “diagonal” operator defined by

$$Q_{B_X}^{00} := P_{B_X}^0 Q_X P_{B_X}^0 \quad (2.38)$$

$Q_{B_X}^{01}$ is an “off-diagonal” operator given by

$$Q_{B_X}^{01} := P_{B_X}^0 Q_X P_{B_X}^1 + P_{B_X}^1 Q_X P_{B_X}^0 \quad (2.39)$$

and $Q_{B_X}^R$ is the remainder

$$Q_{B_X}^R := P_{B_X}^2 Q_X P_{B_X}^2 + P_{B_X}^1 Q_X P_{B_X}^1 \quad (2.40)$$

Note that, since $Q_X \in \mathcal{A}_X$, the operators $P_{B_X}^i Q_X P_{B_X}^2$ and $P_{B_X}^2 Q_X P_{B_X}^i$ vanish, for $i=0, 1$.

Using the decomposition (2.37) we can write the Hamiltonian H_A as follows:

$$H_A = H_{0A} + V_A^{00} + V_A^{01} + V_A^R \quad (2.41)$$

where $V_A^{00} = \sum_{X \subset A} Q_{B_X}^{00}$, $V_A^{01} = \sum_{X \subset A} Q_{B_X}^{01}$, and $V_A^R = \sum_{X \subset A} Q_{B_X}^R$.

There is a slight subtlety, at this point, related to *boundary conditions*: The definition of the operators $P_{B_X}^i$, $i=0, 1, 2$, and of $Q_{B_X}^{00}$, $Q_{B_X}^{01}$, $Q_{B_X}^R$ for regions X with the property that $B_X \cap A^c$ is *non-empty* must, in general, be modified in such a way that the boundary conditions imposed on the configurations on A^c are properly taken into account. We shall not enter into a detailed discussion of this (primarily technical and usually straightforward) issue. In fact, we shall usually think of periodic boundary conditions for which the issue does not arise.

For notational simplicity we henceforth suppress the subscript A . Following the guidelines explained in the Introduction, we search to eliminate the first-order off-diagonal terms $Q_{B_X}^{01}$, through a unitary transformation $U^{(1)}(\lambda) = \exp(S_1(\lambda))$, where $S_1(\lambda)$ is of degree 1 and is given by a sum of local operators:

$$S_1(\lambda) := \sum_X S_{1B_X}(\lambda) \quad (2.42)$$

In the sequel we shall also suppress the explicit λ -dependence of the operators $S_1(\lambda)$ and $S_{1B_X}(\lambda)$. In order to gain mathematical control of the resulting expressions, it is essential⁽¹²⁾ that each S_{1B_X} be a *local* operator.

By the Lie–Schwinger series (2.31), the unitary operator $U^{(1)}$ yields the transformed Hamiltonian

$$\begin{aligned} H^{(1)} &:= e^{S_1} H e^{-S_1} \\ &= H_0 + V^{00} + V^{01} + V^R \\ &\quad + \sum_{n \geq 1} \frac{1}{n!} \text{ad}^n S_1 (H_0 + V^{00} + V^{01} + V^R) \end{aligned} \quad (2.43)$$

To leading order, the operators S_1 , V^{00} , V^{01} and V^R depend linearly on the perturbation parameter λ . We wish to eliminate V^{01} . This leads to the condition

$$\text{ad } H_0(S_1) = V^{01} \quad (2.44)$$

If this equation is satisfied, the Hamiltonian (2.43) becomes—singling out the terms up to second order in λ —

$$H^{(1)} = H_0 + V^{00} + V^R + V_2 + \sum_{n \geq 2} \frac{1}{n!} \text{ad}^n S_1 \left(V^{00} + V^R + \frac{n}{n+1} V^{01} \right) \quad (2.45)$$

with

$$V_2 := \text{ad } S_1 \left(V^{00} + V^R + \frac{V^{01}}{2} \right) \quad (2.46)$$

Condition (2.44) reads

$$\sum_X \text{ad } H_0(S_{1B_X}) = \sum_X Q_{B_X}^{01} \quad (2.47)$$

which, given (2.35), suggests the choice $S_{1B_X} = \text{ad}^{-1} H_0(Q_{B_X}^{01})$. The locality of the operator S_{1B_X} follows from (2.30), which implies that

$$\text{ad}^{-1} H_0(Q_{B_X}^{01}) = \text{ad}^{-1} \bar{H}_{0X}(Q_{B_X}^{01}) \quad (2.48)$$

This is because the operator $Q_{B_X}^{01}$ vanishes on all states which are *not* local ground states for $H_{0B_X \setminus X}$ (see (2.6) and (2.17)), whereas $\bar{H}_{0B_X^c}$ measures the energy of the configuration outside X ; see definition (2.29). Hence, (2.47) is satisfied if we choose

$$S_{1B_X} = \text{ad}^{-1} \bar{H}_{0X}(Q_{B_X}^{01}) \quad (2.49)$$

Selfadjointness of \bar{H}_{0X} and $Q_{B_X}^{01}$ implies anti-selfadjointness of S_{1B_X} and hence of S_1 . The identities (2.42) and (2.49) show that S_1 is given by a sum of local operators. The condition that S_{1B_X} should be a local operator (i.e., $S_{1B_X} \in \mathcal{A}_{B_X}$) motivates our introduction of the “protection zone” $B_X \setminus X$. In ref. 12 it is shown that the family $\{S_{1B_X}\}$ satisfies the required summability condition if the initial interaction $\{Q_X\}$ does.

More precisely, if P^i denotes the projection onto the *eigenspace* of \bar{H}_{0X} corresponding to an eigenvalue E_i , $E_0 = 0 < E_1 < E_2 < \dots$, then from (2.34)

$$S_{1B_X} = \sum_{ij} P^i \frac{Q_{B_X}^{01}}{E_i - E_j} P^j \tag{2.50}$$

For $Q_{B_X}^{01}$ as in (2.39), $i \neq j$ (and either $i = 0$, or $j = 0$); thus $E_i - E_j \neq 0$. Hence S_{1B_X} is a well defined operator. Let us point out that, with these definitions,

$$\begin{aligned} V_2 &= \sum_{\substack{X_1, X_2 \\ B_{X_1} \cap X_2 \neq \emptyset}} \text{ad } S_{1B_{X_1}} \left(Q_{B_{X_2}}^{00} + Q_{B_{X_2}}^R + \frac{Q_{B_{X_2}}^{01}}{2} \right) \\ &=: \sum_{\substack{X_1, X_2 \\ B_{X_1} \cap X_2 \neq \emptyset}} V_{2B_{X_1 \cup X_2}} \end{aligned} \tag{2.51}$$

The transformed Hamiltonian (2.43) can be written in the form

$$H^{(1)} = K^{(1)} + R^{(1)} \tag{2.52}$$

where the operator $K^{(1)}$ contains the leading-order block-diagonal contributions:

$$K^{(1)} = H_0 + V^{00} + V^R + V_2^{00} + V_2^R \tag{2.53}$$

where the last two terms are sums of operators

$$V_{2B_{X_1 \cup X_2}}^{00} := P_{B_{X_1 \cup X_2}}^0 V_{2B_{X_1 \cup X_2}} P_{B_{X_1 \cup X_2}}^0 \tag{2.54}$$

$$V_{2B_{X_1 \cup X_2}}^R := P_{B_{X_1 \cup X_2}}^1 V_{2B_{X_1 \cup X_2}} P_{B_{X_1 \cup X_2}}^1 + P_{B_{X_1 \cup X_2}}^2 V_{2B_{X_1 \cup X_2}} P_{B_{X_1 \cup X_2}}^2 \tag{2.55}$$

This leading part $K^{(1)}$ basically corresponds to the first-order expressions usually presented in the literature on perturbation expansions. The “remainder” $R^{(1)}$, on the other hand, starts with the leading “non-diagonal” terms and includes all higher-order contributions arising from the Lie-Schwinger series (2.43)

$$\begin{aligned} R^{(1)} &= V_2^{01} + \sum_{n \geq 2} \sum_{\substack{X_0, X_1, \dots, X_n: \\ X_0 \cup \dots \cup X_n = \text{c.s.}}} \frac{1}{n!} \\ &\times \text{ad } S_{1B_{X_n}} \left(\text{ad } S_{1B_{X_{n-1}}} \left(\dots \left(Q_{B_{X_0}}^{00} + Q_{B_{X_0}}^R + \frac{n}{n+1} Q_{B_{X_0}}^{01} \right) \dots \right) \right) \end{aligned} \tag{2.56}$$

where $X_0 \cup \dots \cup X_n \equiv \text{c.s.}$ denotes the condition

$$X_i \cap B_{Y_{i-1}} \neq \emptyset \quad \text{for } 1 \leq i \leq n \quad (2.57)$$

with $Y_{i-1} = X_0 \cup \dots \cup X_{i-1}$, and

$$V_{2B_{X_1 \cup X_2}}^{01} := P_{B_{X_1 \cup X_2}}^0 V_{2B_{X_1 \cup X_2}} P_{B_{X_1 \cup X_2}}^1 + P_{B_{X_1 \cup X_2}}^1 V_{2B_{X_1 \cup X_2}} P_{B_{X_1 \cup X_2}}^0 \quad (2.58)$$

As shown in ref. 12, the series (2.56) converges, in fact absolutely and exponentially fast, if the original interaction Q satisfies (2.20).

In fact, the transformed Hamiltonian $H^{(1)}$ comes from an interaction

$$\Phi^{(1)} = \Psi_0^{(1)} + \tilde{Q}^{(1)} \quad (2.59)$$

where $\Psi_0^{(1)}$ and $\tilde{Q}^{(1)}$ are the interactions whose terms yield $K^{(1)}$ and $R^{(1)}$ respectively. Explicitly, $\Psi_0^{(1)} = \{ \Psi_{0B_Y}^{(1)} \}$ where the $\Psi_{0B_Y}^{(1)}$ are nonzero only for $Y = X$ or $Y = X_1 \cup X_2$ with $B_{X_1} \cap X_2 \neq \emptyset$ and X, X_1, X_2 (original) bonds and take the values

$$\Psi_{0B_X}^{(1)} = P_{B_X}^0 \Phi_{0X} P_{B_X}^0 + P_{B_X}^1 \Phi_{0X} P_{B_X}^1 + Q_{B_X}^{00} + Q_{B_X}^R + V_{2B_X}^{00} + V_{2B_X}^R \quad (2.60)$$

$$\Psi_{0B_{X_1 \cup X_2}}^{(1)} = V_{2B_{X_1 \cup X_2}}^{00} + V_{2B_{X_1 \cup X_2}}^R \quad (2.61)$$

All the operators involved are “diagonal” with respect to the partition of unity (2.36) or the analogous partition with X replaced by $X_1 \cup X_2$. The interaction $\tilde{Q}^{(1)}$ has only terms of the form $\{ \tilde{Q}_{B_Y}^{(1)} \}$, where Y is a “c.s.”-connected set of quantum bonds:

$$Y = \bigcup_{j=0}^n X_j \equiv \text{c.s.}, \quad n \geq 1 \quad (2.62)$$

and

$$\tilde{Q}_{B_Y}^{(1)} = \begin{cases} V_{2B_{X_0 \cup X_1}}^{01} & n = 1 \\ \frac{1}{n!} \text{ad } S_{1B_{X_n}} \left(\text{ad } S_{1B_{X_{n-1}}} \left(\dots \left(Q_{B_{X_0}}^{00} + Q_{B_{X_0}}^R + \frac{n}{n+1} Q_{B_{X_0}}^{01} \right) \dots \right) \right) & n \geq 2 \end{cases} \quad (2.63)$$

The analysis of ref. 12 shows that the operators $\tilde{Q}_Z^{(1)}$, which make up the remainder $R^{(1)}$, decay exponentially in the size of their supports. More precisely, there exists a positive constant $r_1 > 0$ such that

$$\sum_{Z \geq 0} \sqrt{\text{tr}[\tilde{Q}_Z^{(1)*}(\lambda) \tilde{Q}_Z^{(1)}(\lambda)]} e^{r_1 s(Z)} = O(\lambda^2) \quad (2.64)$$

where $s(Z)$ denotes the cardinality of the smallest connected subset of the lattice containing Z . Furthermore, the part of (2.64) involving “00”-components is of order 3 or larger in λ . It is, therefore, natural to expect that this interaction $\{\tilde{Q}_{B_Y}^{(1)}\}$ does not contribute to the ground-state energy of the transformed Hamiltonian $H^{(1)}$, to second order in the perturbation parameter λ . This fact is easy to see in finite volume, but, as mentioned before, its verification in the thermodynamic limit—at the level of energy densities—requires a suitable construction of (infinite-volume) ground states. For this reason we shall be able to confirm this expectation only in those cases where the transformed interaction satisfies the hypotheses of the quantum Pirogov–Sinai theory of Section 4.2. (This excludes models with a continuous symmetry.)

These remarks motivate the customary decomposition of $\Psi_0^{(1)}$ into the “00” or “low energy” sector and the rest:

$$\begin{aligned}\Psi_{0B_Y}^{(1)} &= [\Psi_{0B_Y}^{(1)}]^{00} + \Omega_{B_Y}^{(1)} \\ &:= \Phi_{0B_Y}^{(1)} + \Omega_{B_Y}^{(1)}\end{aligned}\tag{2.65}$$

It is worth noting that the interaction $\Phi_0^{(1)}$ is of *finite range*. The methods discussed in Section 4 for the study of the phase diagram rely on the choice of a suitable tensor product basis $\{e(\omega)\}$ such that the operators $\Phi_{0B_Y}^{(1)}$ can be further decomposed into a part that is *exactly* diagonal in the tensor product basis $\{e(\omega)\}$ —i.e., is “*classical*” with respect to $\{e(\omega)\}$ —and a small perturbation. The optimal choice of $\{e(\omega)\}$ is the one that renders this perturbation as small as possible.

With (2.65) we obtain

$$\Phi^{(1)} = \Phi_0^{(1)} + Q^{(1)}\tag{2.66}$$

where $\Phi_0^{(1)} = \{\Phi_{0B_Y}^{(1)}\}$ and $Q^{(1)} = \{\tilde{Q}_{B_Y}^{(1)} + \Omega_{B_Y}^{(1)}\}$. Usually, in the physics literature, only the leading part $\Phi_0^{(1)}$ is reported, expecting that it is responsible for the decisive contribution to the ground state energy of the transformed interaction $\Phi^{(1)}$, to second order in the perturbation parameter λ . One expects to gain heuristic insight into the structure of ground- and low-temperature states of Φ from the ground states of $\Phi_0^{(1)}$. For example, large degeneracies in the spectrum of the Hamiltonian determined by Φ_0 may turn out to be lifted in the spectrum of the one determined by $\Phi_0^{(1)}$. In particular, the classical part of this last interaction ought to lead to a more accurate insight into low-temperature properties of the system than the original Φ_0 . The examples below illustrate instances where these expectations can be rigorously confirmed.

2.4. Second-Order Perturbation Theory

Next, we search for a unitary transformation which removes the off-diagonal part of the original perturbation, $\{Q_{B_Y}^{01}\}$, to order $|\lambda|^2$. A possible approach (certainly not the only one, see the discussion in Section 2.5 below), is to transform the interaction $\Phi^{(1)}$ so as to eliminate the lowest order off-diagonal part of the perturbation $Q^{(1)}$. This leads one to consider a unitary transformation of the form

$$U^{(2)}(\lambda) = e^{S_2(\lambda)} e^{S_1(\lambda)} \quad (2.67)$$

where $S_1 \equiv S_1(\lambda) = \sum_{X \subset \mathcal{A}} S_{1B_X}$ is defined by (2.49), while $S_2(\lambda)$ is determined from the above requirement. The generator $S_2(\lambda)$ must have leading terms of degree 2 and is required to be a sum of local operators:

$$S_2 \equiv S_2(\lambda) = \sum_{Y \subset \mathcal{A}} S_{2B_Y}(\lambda) \quad (2.68)$$

We notice that the choice (2.67) does *not* amount to an iteration of the first-order procedure, because we keep using the partitions of unity determined by the spectral projections of the *original* classical part Φ_0 , rather than those corresponding to the transformed $\Phi_0^{(1)}$. We comment in Section 2.5, below, how an iterated method (Method 3) would proceed.

To alleviate the forthcoming formulas let us suppress the explicit λ -dependence of the operators $S_1(\lambda)$ and $S_2(\lambda)$. The unitary transformation yields the Hamiltonian

$$\begin{aligned} H^{(2)} &:= e^{S_2} e^{S_1} H e^{-S_1} e^{-S_2} \\ &= e^{S_2} H^{(1)} e^{-S_2} \end{aligned} \quad (2.69)$$

where $H^{(1)}$ is the Hamiltonian given by (2.45). Applying the Lie–Schwinger series we see that the term V_2^{01} can be removed by defining

$$\begin{aligned} S_2 &:= \text{ad}^{-1} H_0(V_2^{01}) \\ &= \sum_{\substack{X_1, X_2 \\ X_1 \cap B_{X_2} \neq \emptyset}} \text{ad}^{-1} \bar{H}_{0X_1 \cup X_2}(V_{2B_{X_1 \cup X_2}}^{01}) \\ &:= \sum_{\substack{X_1, X_2 \\ X_1 \cap B_{X_2} \neq \emptyset}} S_{2B_{X_1 \cup X_2}} \end{aligned} \quad (2.70)$$

With this choice, we obtain—singling out the terms of up to fourth order in λ —

$$H^{(2)} = H_0 + V^{00} + V^R + V_2^{00} + V_2^R + V_3 + V_4 + T \quad (2.71)$$

where

$$V_3 = \text{ad}^2 S_1 \left(\frac{V^{00}}{2} + \frac{V^R}{2} + \frac{2V^{01}}{3!} \right) + \text{ad} S_2 \left(V_2^{00} + V_2^R + \frac{V_2^{01}}{2} \right) \quad (2.72)$$

$$V_4 = \text{ad}^3 S_1 \left(\frac{V^{00}}{3!} + \frac{V^R}{3!} + \frac{3V^{01}}{4!} \right) \quad (2.73)$$

and T consists of all terms of order n with $n \geq 5$.

The transformed Hamiltonian $H^{(2)}$ can be written as

$$H^{(2)} = K^{(2)} + R^{(2)} \quad (2.74)$$

where

$$K^{(2)} = K^{(1)} + V_3^{00} + V_3^R + V_4^{00} + V_4^R \quad (2.75)$$

is given entirely in terms of an interaction $\Psi_0^{(2)} \equiv \{ \Psi_{0B_Y}^{(2)} \}$, with the property that the operators $\Psi_{0B_Y}^{(2)}$ are “diagonal” with respect to the partitions of unity

$$\mathbf{1} = P_{B_Y}^0 + P_{B_Y}^1 + P_{B_Y}^2 \quad (2.76)$$

and are of order k in λ , with $0 \leq k \leq 4$. All terms which are “off-diagonal”—starting with $V_3^{01} + V_4^{01}$ —, and all “diagonal” terms of higher orders, are included in the remainder $R^{(2)}$, which is given in terms of an interaction $\tilde{Q}^{(2)} = \{ \tilde{Q}_{B_Y}^{(2)} \}$. The analysis of ref. 12 shows that these operators satisfy

$$\sum_{Z \geq 0} \sqrt{\text{tr}[\tilde{Q}_Z^{(2)*}(\lambda) \tilde{Q}_Z^{(2)}(\lambda)]} e^{r_2 s(Z)} = O(\lambda^3) \quad (2.77)$$

for some $r_2 > 0$, and that a similar sum involving “00”-components is of order 5 or larger in λ .

Further, as in (2.65), we can write

$$\Psi_0^{(2)} = \Phi_0^{(2)} + \Omega_0^{(2)} \quad (2.78)$$

where $\Phi_0^{(2)} \equiv \{\Phi_{0B_Y}^{(2)}\}$ is a finite range interaction with the property that $[\Phi_0^{(2)}]^{ij} = 0$, for $ij \neq 00$. One expects this part to determine the ground-state energy *to order 4 in λ* .

2.5. Synopsis of Perturbation Theory

The above procedure can be iterated to any finite order in λ . To n th order, we aim at constructing a unitary operator, $U_A^{(n)}(\lambda)$, such that

$$H_A^{(n)}(\lambda) = U_A^{(n)}(\lambda) H_A(\lambda) U_A^{(n)}(\lambda)^* \quad (2.79)$$

has the property that

$$H_A^{(n)}(\lambda) = \sum_{Z \subset A} \Phi_Z^{(n)}(\lambda) \quad (2.80)$$

with

$$P_{B_Z}^0 \Phi_Z^{(n)}(\lambda) P_{B_Z}^1 + P_{B_Z}^1 \Phi_Z^{(n)}(\lambda) P_{B_Z}^0 = O(|\lambda|^{n+1}) \quad (2.81)$$

for all Z . We need to ensure that the conjugation of an interaction with exponential decay by the operator $U_A^{(n)}(\lambda)$ is again an interaction with exponential decay. In ref. 12 we present two possible structures for an operator $U_A^{(n)}(\lambda)$ compatible with this requirement (we drop the subscript A):

Method 1:

$$U_A^{(n)}(\lambda) = e^{S_n^{(1)}(\lambda)} \dots e^{S_1^{(1)}(\lambda)} \quad (2.82)$$

Method 2:

$$U_A^{(n)}(\lambda) = \exp\left(\sum_{j=1}^n S_j^{(2)}(\lambda)\right) \quad (2.83)$$

In both cases,

$$S_j^{(\alpha)}(\lambda) = \sum_Z S_{jZ}^{(\alpha)}(\lambda), \quad \alpha = 1 \text{ or } 2 \quad (2.84)$$

where the local operators $S_{jZ}^{(\alpha)}(\lambda)$ are of degree j in λ . The idea is to determine these operators *recursively* in such a way that the condition (2.81) holds, for $n = 1, 2, 3, \dots$. Given $S_{1Y}^{(\alpha)}, \dots, S_{kY}^{(\alpha)}$, for arbitrary Y , (2.81) uniquely fixes the “off-diagonal” contribution to $S_{k+1Z}^{(\alpha)}$, for any Z and for any $k < n$.

Explicit formulas may be found in ref. 12. The method described in Section 2.4 follows method 1.

There is a third way of organizing the recursive perturbative construction of unitary operators $U^{(n)}(\lambda)$ approximately block-diagonalizing the Hamiltonian H , inspired by Newton's method and similar, in spirit, to the renormalization group strategy. Recall that first order perturbation theory [see (2.66) in Section 2.3] yields a unitary operator $U^{(1)}(\lambda)$ such that

$$U^{(1)}(\lambda) H U^{(1)}(\lambda)^* =: H^{(1)} = H_0^{(1)} + V^{(1)} \quad (2.85)$$

where $H_0^{(1)} = \sum_Y \Phi_{0B_Y}^{(1)}$, $\Phi_0^{(1)} = \{\Phi_{0B_X}^{(1)}\}$ is a block-diagonal interaction, and the interaction giving rise to $V^{(1)} := \sum_Y Q_{B_Y}^{(1)}$ has "off-diagonal" terms of order 2 in λ . The third method to construct the conjugations is based on keeping track of the low-energy spectrum of the Hamiltonians determined by $\{\Phi_{0B_Y}^{(1)}\}$ (rather than by $\{\Phi_{0B_Y}\}$), and, in particular, of their ground states. This gives rise to a partition of unity

$$\mathbf{1} = {}^{(1)}P_{B_X}^0 + {}^{(1)}P_{B_X}^1 + {}^{(1)}P_{B_X}^2 \quad (2.86)$$

which serves to decompose the operators $Q_X^{(1)}$ into

$$Q_X^{(1)} = [Q_X^{(1)}]^{00} + [Q_X^{(1)}]^{01} + [Q_X^{(1)}]^R \quad (2.87)$$

as in (2.37), and hence

$$H^{(1)} = H_0^{(1)} + [V^{(1)}]^{00} + [V^{(1)}]^{01} + [V^{(1)}]^R \quad (2.88)$$

in analogy to (2.41). We now proceed as in (2.42) through (2.50) of Section 2.3. This yields an operator

$$S_2^{(3)}(\lambda) = \sum_X S_{2B_X}^{(3)}(\lambda) \quad (2.89)$$

such that

$$H^{(2)} = e^{S_2^{(3)}} H^{(1)} e^{-S_2^{(3)}} \quad (2.90)$$

has the form

$$H^{(2)} = H_0^{(2)} + V^{(2)} \quad (2.91)$$

where the perturbation $V^{(2)}$ does not have any "off-diagonal" terms of order ≤ 2 , with respect to the partition of unity (2.86). We may now

proceed recursively, in the same manner, eliminate off-diagonal terms to ever higher order in λ .

The analysis of ref. 12 remains valid for this case too, and provides proofs of convergence and summability of the different interactions.

3. PERTURBATION EXPANSION FOR THE ONE-BAND HUBBARD MODEL NEAR HALF-FILLING

3.1. Preliminary Remarks

In this section we derive the effective Hamiltonians for the one-band Hubbard model, defined by the Hamiltonian (1.1), near half-filling by applying the perturbative unitary conjugation, Method 1, described in Section 2.5. This model has a number of simplifying features that makes it ideal for a non-trivial exemplary application of our methods. The simplifications stem from the fact that its leading classical interaction [formula (3.3) below] is a sum of on-site terms. First, this implies that every eigenvalue of H_{0X} , $X \subset \mathcal{A}$ [defined as in (2.28)], is a sum of on-site energies $\varepsilon_x(s)$ [where s denotes the on-site configuration and $x \in \mathcal{A}$] which for this model are

$$\varepsilon_x(\uparrow) = -\mu_+, \quad \varepsilon_x(\downarrow) = -\mu_-, \quad \varepsilon_x(\emptyset) = 0, \quad \varepsilon_x(\uparrow, \downarrow) = U - \mu_+ - \mu_- \quad (3.1)$$

Hence its zero-temperature phase diagram is easy to determine (Fig. 1).

Second, the classical interaction has range $R=0$, and there is no need for protection zones:

$$B_Y = Y \quad (3.2)$$

for arbitrary $Y \subset \mathcal{A}$.

Below we shall consider, for the whole shaded region of Fig. 2, projections onto the entire band of single-occupancy states. These states are all simultaneously (local) ground states of the classical interaction along the line $\mu_+ = \mu_-$ (in the complement of this line this degeneracy tends to be lifted).

We present the block-diagonalization of the Hubbard Hamiltonian only to second (Section 3.4) and third order (Section 3.5) in the hopping amplitudes. But we believe that the following discussion, together with Section 4 of ref. 12, provide enough details for a motivated reader to pursue the procedure to an arbitrary order.

3.2. The Original Interaction

As mentioned in the Introduction, it is necessary to implement our perturbation scheme at the level of interactions instead of Hamiltonians. The dominant term, H_{0A} , of the Hamiltonian (1.1) can be expressed in terms of an on-site interaction $\Phi_0 = \{\Phi_{0x}\}$ where

$$\Phi_{0x} = Un_{x+}n_{x-} - \frac{h}{2}(n_{x+} - n_{x-}) - \frac{k}{2}(n_{x+} + n_{x-}) \quad (3.3)$$

with $x \in A$ and

$$h := \mu_+ - \mu_-, \quad k := \mu_+ + \mu_- \quad (3.4)$$

As in (2.28), this interaction defines local Hamiltonians

$$H_{0Y} = \sum_{x \in Y} \Phi_{0x} \quad (3.5)$$

The quantum perturbation is the kinetic-energy term, and the perturbation parameters are the hopping amplitudes $\underline{t} = \{t_+^b, t_-^b, t_+^{\bar{b}}, t_-^{\bar{b}}\}$, where $b = [xy]$ denotes an ordered pair of nearest neighbor sites and \bar{b} is the same nearest neighbor pair, but with *reverse* ordering. The perturbation is assumed to be translation invariant, that is $t_{\pm b}$ only depends on the direction, $y - x$, of b . We shall write

$$t = \max\{t_+^b, t_-^b, t_+^{\bar{b}}, t_-^{\bar{b}}\} \quad (3.6)$$

We write the quantum interaction as

$$Q_X \equiv Q_X(\underline{t}) = Q_{[xy]}(\underline{t}) + Q_{[yx]}(\underline{t}) \quad (3.7)$$

where X denotes the *unordered* pair $\langle xy \rangle$ and

$$Q_b \equiv Q_b(\underline{t}) = \sum_{\sigma = \pm} Q_{\sigma b}(\underline{t}) \quad (3.8)$$

with

$$Q_{\sigma b} \equiv Q_{\sigma b}(\underline{t}) := t_{\sigma}^b c_{x\sigma}^{\dagger} c_{y\sigma} \quad (3.9)$$

Moreover, if the Hamiltonian is assumed to be self-adjoint then

$$t_{\pm}^b = (t_{\pm}^{\bar{b}})^* \quad (3.10)$$

3.3. The local projections

We start by introducing partitions of unity giving rise to appropriate decompositions of the hopping terms in the Hubbard Hamiltonian into “diagonal” and “off-diagonal” operators. The most interesting part of the shaded region of Fig. 2 is the vicinity of the line of infinite degeneracy. On this line, the ground states of Φ_0 are (linear combinations of) configurations with precisely one (up-spin or down-spin) electron occupying each site. For $Y \subset \mathcal{A}$, the orthogonal projections onto the subspace spanned by the ground states of H_{0Y} are of the form

$$P_Y^0 := \prod_{x \in Y} P_x^0 \quad (3.11)$$

with

$$P_x^0 := (n_{x+} - n_{x-})^2 \quad (3.12)$$

As remarked above, as the classical interaction (3.3) is on-site, i.e., of zero range, there is no need for protection zones. This implies, first, that we can define the projection P_{0Y}^1 by setting

$$\mathbf{1} = P_Y^0 + P_Y^1 \quad (3.13)$$

and, second, that we can use these projections P_Y^0 and P_Y^1 throughout the whole shaded region of Fig. 2. The operators P_Y^0 are projections onto states with single occupancy. This family of states included therefore, ground states and low-lying excitations. The operators P_Y^1 , on the other hand, project onto the complementary subspace corresponding to of high-energy excitations, formed by states with at least one site in Y occupied by zero or two electrons.

3.4. First-Order Perturbation Theory

Let us perform the first step of the perturbative analysis of Section 2, namely the block-diagonalization of the interaction to second order in the perturbation parameters. In this section, X is always used to denote *a pair of nearest neighbor sites*.

We consider the perturbation defined in (3.7)–(3.9) and decompose it into the form (2.37), $Q_X = Q_X^{00} + Q_X^{01} + Q_X^R$, using the projections P_X^0 and P_X^1 defined in (3.11)–(3.12) ($P_Y^2 = 0$ for all $Y \subset \mathcal{A}$). It is simple to check that

$$Q_X^{00} = 0 \quad (3.14)$$

Our goal is to construct a unitary transformation,

$$U^{(1)}(t) = e^{S_1(t)} \quad (3.15)$$

with the property that $H_A^{(1)}(t) := U^{(1)}(t) H_A U^{(1)}(t)^*$ only contains off-diagonal operators of order 2 and higher in t . Following the general ideas discussed in Section 2.3, we attempt to construct an operator $S_1(t)$ of the form

$$S_1(t) = \sum_X S_{1X}(t) = \sum_{\sigma=+,-} \sum_b t_\sigma^b S_{1\sigma b} \quad (3.16)$$

The formulas for the operators $S_{1\sigma b}$ can be inferred from Section 2 [formula (2.49)]:

$$S_{1\sigma\langle xy \rangle} = \text{ad}^{-1} H_{0\{xy\}}(c_{x\sigma}^\dagger c_{y\sigma}) \quad (3.17)$$

Conjugating the Hamiltonian H of the asymmetric single-band Hubbard model by the operator $e^{S_1(t)}$, yields an effective Hamiltonian $H^{(1)}$ [see (2.45)] given in terms of a new interaction, $\Phi^{(1)}$, determined by (2.52)–(2.59) (with $B_X = X$).

If we perform the decomposition (2.65) ff. we obtain, for the Hubbard model, the low-energy-sector leading terms

$$\Phi_{0X}^{(1)} = \begin{cases} P_x^0 \Phi_{0x} P_x^0 & \text{if } X = \{x\} \\ \frac{1}{2} P_X^0 \text{ad } S_{1X}(Q_X^{01}) P_X^0 & \text{if } X \text{ is a pair of n.n.} \end{cases} \quad (3.18)$$

It is not hard to see that the two-bond terms $V_{X_1 \cup X_2}^{00} = \frac{1}{2} [\text{ad } S_{1B_{X_1}}(Q_{B_{X_2}}^{01}) + S_{1B_{X_2}}(Q_{B_{X_1}}^{01})]^{00}$ are zero if $X_1 \neq X_2$. The second line on the R.H.S. Of (3.18) involves operators corresponding to an electron of a particular spin hopping from a singly occupied site to a nearest-neighbor site occupied by an electron of opposite spin, thus momentarily creating a doubly occupied site and a hole. They then restore the condition of single occupancy of the sites by causing one of the electrons on the doubly occupied site to hop to the neighboring hole.

In fact, the interaction (3.18) coincides with the first-order calculations often presented in the literature since the initial observation of Anderson.⁽⁴⁾ It is conveniently expressed in terms of the spin operators

$$\mathbf{S}_x := \sum_{s,s'=+,-} c_{xs}^\dagger \mathbf{S}_{ss'} c_{xs'} \quad (3.19)$$

where $\mathbf{S} \equiv \frac{1}{2}(\sigma^1, \sigma^2, \sigma^3)$ and $\sigma^1, \sigma^2, \sigma^3$ are the standard Pauli matrices. Note that

$$S_x^3 = \frac{1}{2}(n_{x+} - n_{x-}) \quad (3.20)$$

and

$$S_x^\pm := S_x^1 \pm iS_x^2 = c_{x\pm}^\dagger c_{x\mp} \quad (3.21)$$

The operators S_x^+ , $S_x^- = (S_x^+)^*$ and S_x^3 form a basis of a representation of the Lie algebra of $SU(2)$ on the four-dimensional Hilbert space $\mathcal{H}_x = \text{span}\{\emptyset, \uparrow, \downarrow, \uparrow\downarrow\}$. These operators annihilate the subspace spanned by $\{\emptyset, \uparrow\downarrow\}$ and act irreducibly (in the spin-1/2 representation) on the subspace spanned by $\{\uparrow, \downarrow\}$. In particular,

$$P_x^0 S_x^3 P_x^0 = S_x^3, \quad P_x^0 S_x^\pm P_x^0 = S_x^\pm \quad (3.22)$$

The operators $\text{ad } S_{1\sigma\bar{b}}(Q_{\sigma\bar{b}}^{01})$, with $\sigma = +, -$, cause the same electron to hop in both steps of the process, whereas the operators $\text{ad } S_{1\sigma\bar{b}}(Q_{\sigma'b}^{01})$, with $\sigma \neq \sigma'$, cause electrons of opposite spins to hop in the two steps. These processes can be expressed in terms of a sequence of creation and annihilation operators of the up-spin and down-spin electrons

$$\begin{aligned} P_X^0 \text{ad } S_{1\sigma\bar{b}}(Q_{\sigma'b}^{01}) P_X^0 &= -\frac{1}{U} P_X^0 [Q_{\sigma\bar{b}}^{01} Q_{\sigma'b}^{01} + Q_{\sigma'b}^{01} Q_{\sigma\bar{b}}^{01}] P_X^0 \\ &= -\frac{t_{\sigma}^{\bar{b}} t_{\sigma'}^b}{U} P_X^0 [c_{y\sigma}^\dagger c_{x\sigma} c_{x\sigma'}^\dagger c_{y\sigma'} + c_{x\sigma}^\dagger c_{y\sigma} c_{y\sigma'}^\dagger c_{x\sigma'} \\ &\quad + c_{y\sigma'}^\dagger c_{x\sigma'} c_{x\sigma}^\dagger c_{y\sigma} + c_{x\sigma'}^\dagger c_{y\sigma'} c_{y\sigma}^\dagger c_{x\sigma}] P_X^0 \end{aligned} \quad (3.23)$$

For $\sigma = \sigma'$, (3.23) yields

$$\begin{aligned} \sum_{\sigma=+,-} P_X^0 \text{ad } S_{1\sigma X}(Q_{\sigma X}^{01}) P_X^0 &= -\frac{2(|t_+^b|^2 + |t_-^b|^2)}{U} P_X^0 [n_{y+}(1-n_{x+}) + (1-n_{y+})n_{x+}] P_X^0 \\ &= \frac{4(|t_+^b|^2 + |t_-^b|^2)}{U} \left(S_x^3 S_y^3 - \frac{P_X^0}{4} \right) \end{aligned} \quad (3.24)$$

To arrive at (3.24), we have made use of the identities

$$P_X^0 n_{y\sigma}(1-n_{x\sigma}) P_X^0 = P_X^0(1-n_{y(-\sigma)}) n_{x(-\sigma)} P_X^0 \quad (3.25)$$

and

$$P_X^0 [n_{x+} n_{y-} + n_{x-} n_{y+}] P_X^0 = \left[-2S_x^3 S_y^3 + \frac{P_X^0}{2} \right] \quad (3.26)$$

for $X = \{xy\}$. In turn, this last identity follows from (3.20), (3.22) and the relations

$$P_x^0 n_{x\sigma} P_x^0 = P_x^0 (1 - n_{x(-\sigma)}) P_x^0 \quad (3.27)$$

and

$$P_x^0 (n_{x+} + n_{x-}) P_x^0 = P_x^0 \quad (3.28)$$

Similarly, for $\sigma \neq \sigma'$, (3.23) yields

$$\begin{aligned} \sum_{\substack{\sigma, \sigma' = +, - \\ \sigma \neq \sigma'}} \text{ad } S_{1\sigma\bar{\sigma}}(Q_{\sigma\bar{\sigma}}^{01}) &= \frac{2(t_+^{\bar{b}} t_-^b + t_-^{\bar{b}} t_+^b)}{U} [S_y^+ S_x^- + S_y^- S_x^+] \\ &= \frac{4(t_+^{\bar{b}} t_-^b + t_-^{\bar{b}} t_+^b)}{U} P_X^0 [S_x^1 S_y^1 + S_x^2 S_y^2] P_{0X} \end{aligned} \quad (3.29)$$

From (3.18), (3.24) and (3.29) we conclude that $\Phi_{0X}^{(1)}$ is the well known Heisenberg interaction

$$\Phi_{0X}^{(1)} = \begin{cases} -hS_x^3 - \frac{k}{2}, & \text{if } X = \{x\} \\ \frac{2[|t_+^b|^2 + |t_-^b|^2]}{U} \left(S_x^3 S_y^3 - \frac{P_X^0}{4} \right) + \frac{2(t_+^{\bar{b}} t_-^b + t_-^{\bar{b}} t_+^b)}{U} [S_x^1 S_y^1 + S_x^2 S_y^2] \\ \text{if } X \text{ is a pair of n.n.} \end{cases} \quad (3.30)$$

[h and k being defined in (3.4)], and $\Phi_{0X}^{(1)} = 0$, for all other $X \subset \mathbb{Z}^v$.

If the hopping amplitudes depend neither on the direction of the hopping nor on the spin orientation $-t_{\pm b} = t \pm \bar{b} = t$ —then the original Hamiltonian H_A (1.1) is the standard one-band Hubbard Hamiltonian, and the interaction (3.30) is that of an *isotropic* Heisenberg model. This model is difficult to treat rigorously because of its $SU(2)$ symmetry, and it is not surprising that the symmetric Hubbard model lies outside the scope of the methods we discuss in Section 4. For high asymmetry, $|t_+^b| \ll |t_-^b|$, the effective interaction (3.30) corresponds to an antiferromagnetic Ising interaction, perturbed by a small spin-flip term. This interaction exhibits a

first-order phase transition to a Néel phase. This applies in particular to the Falicov Kimball model, for which $t_+^b = 0$ and $t_-^b = t$.

From the discussion of Section 2.3 we know that the other terms of the transformed interaction $\Psi^{(1)}$ are small. The terms corresponding to the rest of $\Psi_0^{(1)}$, called $\Omega^{(1)}$ in (2.65), involve only transitions within the excited band, while the “off-diagonal” remainder is of second order in t [Eq. (2.64)].

3.5. Second-Order Perturbation Theory

To convey the taste of higher order calculations, let us discuss the block diagonalization process to one further order. The objective is to find the interaction $\Phi_0^{(2)}$ of (2.78), that is, $\Phi_0^{(2)} = [\Psi_0^{(2)}]^{00}$, where $\Psi_0^{(2)}$ is the block-diagonal interaction giving rise to $K^{(2)}$ in (2.75). Thus

$$\Phi_0^{(2)} = \Phi_0^{(1)} + \varphi_0^{(2)} \quad (3.31)$$

where $\Phi_0^{(1)}$ was determined in the previous section [formula (3.30)] and $\varphi_0^{(2)}$ is such that $V_3^{00} + V_4^{00} = \sum_Y \varphi_{0Y}^{(2)}$.

Inspection shows that many of the terms comprising $V_3^{00} + V_4^{00}$ are zero when the original perturbation Q is just a nearest-neighbor hopping term. We summarize in Table 1 the non-zero terms of the resulting interaction $\varphi_0^{(2)}$, both in its general form and in the form taken in the case where the hopping constant does not depend on the direction of hopping. Notice the presence of local projectors. They make the interaction well defined, in the sense of being volume-independent. Conceptually, they constitute the main difference between our expressions and similar formulas reported previously in the literature. In a few terms, the local projectors can be omitted because of property (3.22). We have also adopted the standard notation

$$S_x^\perp S_y^\perp := S_x^1 S_y^1 + S_x^2 S_y^2 = \frac{1}{2}(S_x^+ S_y^- + S_x^- S_y^+) \quad (3.32)$$

As a further illustration we present in Table 2 the effective Hamiltonians for the (symmetric) Hubbard and Falicov–Kimball models. The latter is a totally classical interaction with discrete symmetries, and hence suitable for the application of the phase-diagram technology of Section 4. In this table, the symbol $\langle xyz \rangle$ denotes that x and y are nearest neighbor sites and so are y and z , while $\left\{ \begin{smallmatrix} w & z \\ x & y \end{smallmatrix} \right\}$ stands for four sites around a plaquette. Both expressions have been derived previously, except for the use of local projectors. The expression for the Hubbard model has been reported, for instance, in refs. 8 and 45 (where the hopping parameter is allowed to depend on the direction), in ref. 10 (together with higher-order corrections,

Table 1. Second-Order Terms of the Effective Interaction in the Low Energy Sector^a

General case	Case $t_{\pm}^b = t_{\pm}^b = t_{\pm}$
$\frac{1}{8} P_X^0 [\text{ad } S_{1X} (\text{ad } S_{1X'} (\text{ad } S_{1X} (Q_X^{01})))] P_X^0$	$-\frac{2(t_+^4 + t_-^4 + 6t_+^2 t_-^2)}{U^3} \left(S_x^3 S_y^3 - \frac{P_{\{x,y\}}^0}{4} \right)$ $-\frac{8(t_+^3 t_- + t_-^3 t_+)}{U^3} S_x^{\perp} S_y^{\perp}$
$P_{X \cup X'}^0 \left[\frac{1}{8} \sum_{C_6} \text{ad } S_{1X_1} (\text{ad } S_{1X_2} (\text{ad } S_{1X_3} (Q_{X_1}^{01}))) \right.$ $\left. + \frac{1}{2} \sum_{C_4} \text{ad } S_{2(X_4 \cup X_3)} (Q_{2(X_1 \cup X_2)}^{01}) \right] P_{X \cup X'}^0$	$-P_{\{x,y,z\}}^0 \left[\frac{2(t_+^2 - t_-^2)^2}{U^3} \left(S_x^3 S_y^3 + S_y^3 S_z^3 - S_x^3 S_z^3 - \frac{1}{4} \right) \right.$ $\left. - \frac{2(t_+^4 + t_-^4)}{U^3} \left(S_x^3 S_z^3 - \frac{1}{4} \right) - \frac{4t_+^2 t_-^2}{U^3} S_x^{\perp} S_z^{\perp} \right] P_{\{x,y,z\}}^0$
$P_{X \cup X' \cup X'' \cup X'''}^0$ $\times \left[\frac{1}{8} \sum_{C_{24}} \text{ad } S_{1X_1} (\text{ad } S_{1X_2} (\text{ad } S_{1X_3} (Q_{X_1}^{01}))) \right.$ $\left. + \frac{1}{2} \sum_{\tilde{C}_4} \text{ad } S_{2(X_4 \cup X_3)} (Q_{2(X_1 \cup X_2)}^{01}) \right]$ $\times P_{X \cup X' \cup X'' \cup X'''}^0$	$P_{\{x,y,z,w\}}^0 \left\{ \frac{40(t_+^4 + t_-^4)}{U^3} S_x^3 S_y^3 S_z^3 S_w^3 \right.$ $-\frac{2(t_+^4 + t_-^4)}{U^3} \left(S_x^3 S_y^3 + \text{c.p.} + S_x^3 S_z^3 + S_y^3 S_w^3 - \frac{1}{4} \right)$ $+ \frac{8(t_+^3 t_- + t_-^3 t_+)}{U^3} \left[5(S_y^{\perp} S_z^{\perp}) S_x^3 S_w^3 + \text{c.p.} \right.$ $\left. - \frac{1}{4} (S_x^{\perp} S_y^{\perp} + \text{c.p.}) \right]$ $+ \frac{40t_+^2 t_-^2}{U^3} (S_x^+ S_y^- S_z^+ S_w^- + S_x^- S_y^+ S_z^- S_w^+)$ $- \frac{4t_+^2 t_-^2}{U^3} [20(S_x^{\perp} S_z^{\perp}) S_y^3 S_w^3$ $+ 20(S_y^{\perp} S_w^{\perp}) S_x^3 S_z^3 + S_x^{\perp} S_z^{\perp} + S_y^{\perp} S_w^{\perp}] \left. \right\} P_{\{x,y,z,w\}}^0$

^a Expressions are given for the relevant orders of the general formula (2.63) (leftmost column) and for the particular case of the Hubbard model with direction-independent hopping (rightmost column). *First line:* $X = \langle xy \rangle$. *Second line:* $X = \langle xy \rangle$, $X' = \langle yz \rangle$, C_6 is the set of sequences (X_1, X_2, X_3, X_4) such that two of its members coincide with X and the remaining ones with X' . C_4 is the subset of C_6 formed by the sequences (X, X', X, X') , (X, X', X', X) or their X to X' permutations. *Third line:* $X = \langle xy \rangle$, $X' = \langle yz \rangle$, $X'' = \langle zw \rangle$, $X''' = \langle wx \rangle$, C_{24} is the set of sequences (X_1, X_2, X_3, X_4) coinciding with (X, X', X'', X''') or any one of its permutations, \tilde{C}_4 is the set of sequences (X_1, X_2, X_3, X_4) coinciding with (X, X', X'', X''') or any one of its cyclic permutations. “c.p.” means “cyclic permutations” obtained by $x \rightarrow y \rightarrow z \rightarrow w \rightarrow x$.

Table 2. Second-Order Effective Hamiltonians in the Low Energy Sector for the Hubbard ($t_+ = t_- = t$) and Falicov–Kimball ($t_+ = 0, t_- = t$) Models

One-band Hubbard	$ \begin{aligned} & -\sum_x \left(hS_x^3 + \frac{k}{2} P_x^0 \right) + \left(\frac{4t^2}{U} - \frac{16t^4}{U^3} \right) \sum_{\langle xy \rangle} \left(\mathbf{S}_x \cdot \mathbf{S}_y - \frac{P_{\{x,y\}}^0}{4} \right) \\ & + \frac{4t^4}{U^3} \sum_{\langle xyz \rangle} P_{\{x,y,z\}}^0 \left(\mathbf{S}_x \cdot \mathbf{S}_z - \frac{1}{4} \right) P_{\{x,y,z\}}^0 \\ & - \frac{4t^4}{U^3} \sum_{\{x,y,z,w\}} P_{\{x,y,z,w\}}^0 \left(\mathbf{S}_x \cdot \mathbf{S}_y + \text{c.p.} + \mathbf{S}_x \cdot \mathbf{S}_z + \mathbf{S}_y \cdot \mathbf{S}_w - \frac{1}{4} \right) P_{\{x,y,z,w\}}^0 \\ & + \frac{80t^4}{U^3} \sum_{\{x,y,z,w\}} [(\mathbf{S}_x \cdot \mathbf{S}_y)(\mathbf{S}_z \cdot \mathbf{S}_w) + (\mathbf{S}_x \cdot \mathbf{S}_w)(\mathbf{S}_y \cdot \mathbf{S}_z) - (\mathbf{S}_x \cdot \mathbf{S}_z)(\mathbf{S}_y \cdot \mathbf{S}_w)] \end{aligned} $
Falicov–Kimball	$ \begin{aligned} & -\sum_x \left(hS_x^3 + \frac{k}{2} P_x^0 \right) + \left(\frac{2t^2}{U} - \frac{2t^4}{U^3} \right) \sum_{\langle xy \rangle} \left(S_x^3 S_y^3 - \frac{P_{\{x,y\}}^0}{4} \right) \\ & - \frac{2t^4}{U^3} \sum_{\langle xyz \rangle} P_{\{x,y,z\}}^0 (S_x^3 S_y^3 + S_y^3 S_z^3 - 2S_x^3 S_z^3) P_{\{x,y,z\}}^0 \\ & - \frac{2t^4}{U^3} \sum_{\{x,y,z,w\}} P_{\{x,y,z,w\}}^0 (S_x^3 S_y^3 + \text{c.p.} + S_x^3 S_z^3 + S_y^3 S_w^3) P_{\{x,y,z,w\}}^0 \\ & + \frac{40t^4}{U^3} \sum_{\{x,y,z,w\}} S_x^3 S_y^3 S_z^3 S_w^3 \end{aligned} $

up to eighth order) and in ref. 37. Our contribution amounts to showing that if one systematically uses local projections, unlike in the first three references, the remainder term in a perturbative block diagonalization of the Hamiltonian can be controlled rigorously. This is our new result. It is an illustration of our general results of ref. 12.

The second-order effective classical Hamiltonian for the Falicov–Kimball model and its ground states, were studied in ref. 31. In ref. 23 a more general expression was obtained involving hopping amplitudes that depend on the direction: $t^{[yx]} = t^{[yx]}* = |t^{[yx]}| e^{i\theta_{xy}}$, $\theta_{xy} = -\theta_{yx}$. Such complex hopping amplitudes describe the influence of a magnetic field. Our expansion methods provide systematic control of remainder terms.

3.6. Higher-Order Perturbation Theory

While straightforward, in principle, the computation of higher-order transformed interactions is a tedious and error-prone process. (In fact, already the second order computations lead to monstrous expressions if

hopping is allowed to depend on the direction as well as spin.) The use of computer codes to perform symbolic algebra becomes mandatory. To encourage industrious readers, we sketch some basic elements of the algebra needed to treat the resulting expressions.

The different terms arising are products of two types of operators: (i) creation and destruction operators, and (ii) projections. We can therefore classify the relevant terms in three categories.

3.6.1. Products of Creation and Destruction Operators. The algebraic manipulations of these operators are well known: one uses the anti-commutation relations (2.9)–(2.10) to obtain expressions in terms of the occupation numbers $n_{x\sigma} = c_{x\sigma}^\dagger c_{x\sigma}$ and the spin operators S_x^\pm defined in (3.21). Furthermore, differences of occupation numbers can be written in terms of S_x^3 via (3.20).

3.6.2. Products of Projections. There is only one equation to consider:

$$P_x^i P_x^j = P_x^i \delta_{ij}, \quad i, j = 0, 1 \quad (3.33)$$

A similar equation holds for projections on any set X . Another pair of potentially useful relations are

$$P_X^0 P_{\tilde{X}}^0 = P_{\tilde{X}}^0, \quad P_X^1 P_{\tilde{X}}^1 = P_X^1 \quad (3.34)$$

whenever $X \subset \tilde{X}$.

3.6.3. Products of Projections and Creation and Destruction Operators. This is the non-trivial part of the algebra. Perhaps, its most important relations are the intertwining relations

$$\begin{aligned} c_{x\sigma} P_x^0 &= P_x^1 c_{x\sigma} & c_{x\sigma} P_x^1 &= P_x^0 c_{x\sigma} \\ c_{x\sigma}^\dagger P_x^0 &= P_x^1 c_{x\sigma}^\dagger & c_{x\sigma}^\dagger P_x^1 &= P_x^0 c_{x\sigma}^\dagger \end{aligned} \quad (3.35)$$

for arbitrary $\sigma = \pm$. They allow a purely algebraic verification of which terms are zero. We remark that projections of the form P_X^1 , with X containing more than one site, are not directly suited for the use of (3.35), because these projections are *not* products of single-site projections. We then use that

$$P_X^1 = 1 - P_X^0 = 1 - \prod_{x \in X} P_x^0 \quad (3.36)$$

As an example, let us sketch the algebraic proof that

$$[\text{ad } S_{1\sigma X}(Q_{\sigma'X'}^{01})]^{00} = 0 \quad (3.37)$$

for $X = \langle xy \rangle$ and $X' = \langle yz \rangle$, with $x \neq z$; a fact only parenthetically mentioned after (3.18). Indeed, the left-hand side of (3.37) is a combination of products of the form

$$P_{\{x, y, z\}}^0 P_{\{x, y\}}^0 c_{y\sigma}^\dagger c_{x\sigma} P_{\{x, y\}}^1 P_{\{y, z\}}^1 c_{z\sigma'}^\dagger c_{y\sigma'} P_{\{y, z\}}^0 P_{\{x, y, z\}}^0 \quad (3.38)$$

plus various $x \leftrightarrow y$ and $y \leftrightarrow z$ permutations. We first notice that the middle projections P_X^1 can be removed. To see this we use (3.36) and then move, for instance, the resulting factors P_y^0 to the far left and far right through the intertwining relations (3.35). Such factors emerge as P_y^1 and cancel with the corresponding factors P_y^0 at both ends [relation (3.33)]. We are left with

$$P_{\{x, y, z\}}^0 c_{y\sigma}^\dagger c_{x\sigma} c_{z\sigma'}^\dagger c_{y\sigma'} P_{\{x, y, z\}}^0 \quad (3.39)$$

where we have also used (3.34). To see that such a term is zero, use again the intertwining relations to show, for instance, that as there is an odd number of creation and annihilation operators involving the site z , the leftmost P_z^0 can be written as P_z^1 on the right. It then annihilates with the corresponding P_z^0 .

There are many other useful relations involving products of projections and creation and destruction operators. Besides the previous formulas (3.22), (3.25), (3.26) and (3.27)/(3.28), we mention

$$n_{x\sigma} P_x^0 = [1 - n_{x(-\sigma)}] P_x^0 \quad (3.40)$$

$$N_{x\sigma} P_x^1 = \frac{n_x}{2} P_x^1 \quad (3.41)$$

and

$$c_{x\sigma'}^\dagger c_{x\sigma}^\dagger P_x^0 = 0 \quad (3.42)$$

$$c_{x\sigma}^\dagger c_{x(-\sigma)} P_x^1 = 0 \quad (3.43)$$

for any $\sigma, \sigma' = \pm$. By the intertwining relations (3.35) the identities (3.40)–(3.43) can also be written with the projections on the right or on the left and the right.

4. LOW-TEMPERATURE PHASE DIAGRAMS

4.1. Foreword on Quantum Pirogov–Sinai Theory

The purposes of Sections 2 and 3 was to construct a unitary operator, $U^{(n)}(\lambda)$, with the property that the conjugated Hamiltonian

$$\begin{aligned} H_A^{(n)}(\lambda) &= U_A^{(n)}(\lambda) H_A(\lambda) U_A^{(n)}(\lambda)^* \\ &= H_{0A}^{(n)}(\lambda) + V_A^{(n)}(\lambda) \end{aligned} \quad (4.1)$$

of some quantum lattice system is “block-diagonal” to order $|\lambda|^{n+1}$. By this we mean that the matrix elements of $V_A^{(n)}(\lambda)$ between ground states, or approximate ground states (low-energy states) of $H_{0A}^{(n)}(\lambda)$ are of order $n+1$. Our method to construct $U_A^{(n)}(\lambda)$ has been (a convergent form of) analytic perturbation theory.

In attempting to gain some insight into the structure of ground states and low-temperature equilibrium states of the Hamiltonian $H_A^{(n)}(\lambda)$, it is tempting to argue that one should neglect the perturbation $V_A^{(n)}(\lambda)$ and study the ground states and low-temperature equilibrium states of $H_{0A}^{(n)}(\lambda)$ —hoping that they are close to those of $H_A^{(n)}(\lambda)$. Unfortunately, this hope is unjustified, in general.

It is a well known fact that arbitrarily small perturbations can have a drastic effect on low-temperature phase diagrams. This is typically the case when the truncated part has an infinite degeneracy. For example, when there is a continuous symmetry, states are usually grouped in bands with gapless intraband excitations. An arbitrarily small additional term can split the lower bands and hence change the phase diagram. Such models are hard to treat rigorously; in particular, no such treatment is available for the (symmetric) Hubbard model, *despite our control on the perturbation series of Section 3*. The case in which the truncated interaction has an infinite degeneracy not connected with a continuous symmetry is usually more tractable. Often, entropy effects (quantum and classical) are the determining aspect, and there exist techniques to deal with them, as we will illustrate below.

The simplest situation arises when the truncated interaction has a zero-temperature phase diagram involving only finite degeneracies. In favorable cases, we expect that each of these ground states gives rise to a corresponding ground state, and a low-temperature state, of the full, untruncated interaction. The detection and description of these phases, however, requires some additional machinery. Indeed, even at zero temperature, where only energy plays a role, we cannot rely on plain diagonalization procedures. First, there is no hope of achieving exact block diagonalization of the

whole *family* of Hamiltonians $\{H_A\}$ needed to pass to the thermodynamic limit, barring miracles (that is, relatively trivial and uninteresting situations). And, second, the estimation of the effect of the “undagonalized” remainders is a delicate matter. The remainder term, $V_A^{(n)}(\lambda)$, makes a negligible contribution to the *energy density*. But it may have a decisive *quantum entropic* effect: It may alter the overall wave function by allowing “virtual quantum transitions” between classical configurations. The situation is even more involved at nonzero temperatures, due to the appearance of thermal fluctuations.

Quantum Pirogov–Sinai Theory. Its bare-bones version^(11,5) applies to systems with a leading part that is “classical,” in the sense of being diagonal in a tensor product basis (Section 2.2). It is based on *contour expansions*. The Duhamel expansion is used to write partition functions and expectations as sums over $(d+1)$ -dimensional piecewise cylindrical surfaces—the $(d+1)$ -st axis corresponding to the inverse temperature (imaginary time) axis. Such “*contours*” have cylindrical pieces, corresponding to Peierls-like contours for the classical part of the interaction, and a finite number of section changes caused by the quantum perturbation. The objective of the theory is to prove that, in the thermodynamic limit, these contours are sparse and far apart. This yields a precise mathematical representation of states as “classical ground states modified by quantum and thermal fluctuations.” In fact, both types of fluctuations are treated on the same footing. So quantum Pirogov–Sinai theory provides a unified description of ground- and low-temperature states.

In brief, the theory establishes sufficient conditions for the energy to dominate over further quantum and thermal entropic effects. As a consequence, the latter can only cause small (and smooth) deformations of the zero-temperature phase diagram of the classical part. That is, the phase diagram remains stable under quantum perturbations and small raises of temperature. This does not mean that all phases remain stable throughout the phase diagram. For instance, small entropic effects can tilt the balance in favor of particular phase(s) of a coexistence region and cause the disappearance of the remaining ones when the thermal or quantum perturbation is switched on. But the theory assures that the unfavored phases reappear for slightly modified parameter values, that is, the perturbed system will also exhibit a coexistence manifold, albeit a little shifted and deformed. Moreover, the theory provides a criterion to determine which phases are stable, and, in fact, it presents a picture of what “stable phase” means. [As a matter of fact, below we shall resort only to this stability criterion. The part on the stability of phase diagrams will not be useful, as coexistence lines will, in all cases, involve infinite degeneracies.]

As we discuss in more detail below, the conditions on the classical part required by the theory are of two types: First, it must lead to finite ground-state degeneracies within the region of interest, and, second, it must satisfy the *Peierls condition* which roughly requires the energy cost of an excitation to be proportional to the area of its boundary. The first requirement forces us to stay away from regions of infinite degeneracy. So, in principle, we would be unable to deal with the line $\mu_+ = \mu_-$ of the phase diagram of Fig. 1. We shall see below that the quantum hopping actually helps us there. Similarly, models with low-cost energy excitations, like the balanced model, are out of reach. In fact, in ref. 16 it is shown how quantum hopping brings this model within reach.

When applicable, the theory does a complete job: It accounts for entropic effects and provides a full description of states. Nevertheless, the theory has a limited scope. In fact, it seems to be applicable only when nothing interesting happens as a result of the perturbation. The hidden card is our perturbation technique. In many instances, it produces a partially diagonalized interaction with a leading classical part incorporating crucial quantum effects. If such a leading part satisfies the right hypotheses, the subsequent application of Pirogov–Sinai theory will prove the existence of phases exhibiting truly quantum-mechanical features. In fact, a slight extension of Pirogov–Sinai is needed in these cases, showing that transitions within the excited band have a negligible effect, regardless of the order. Such an extension, based on a more careful definition of contours that distinguishes “high-to-high” transitions from the rest, is presented in ref. 12. Below, we prove that hopping produces quantum symmetry breaking among the ground states of the on-site Hubbard interaction, which brings the degeneracy down to a finite one. This is an instance of “quantum entropic selection.” Another example, presented in ref. 16, is the “quantum restoration of the Peierls condition” taking place in the balanced model.

Incidentally, the thermal entropic selection is a better known phenomenon, which, in some cases, can trigger a complicated pattern of phases with cascades or staircases of phase transitions. This effect has been the object of extensions of Pirogov–Sinai theory based on the notion of *restricted ensembles*.^(6, 44, 24, 7, 34) The extension of this theory to quantum systems is a promising direction of research. The work in ref. 35 can be considered as a step in this direction, though it does not treat genuinely degenerate quantum interactions and only resorts to restricted ensembles as an alternative way to exhibit degeneracy breaking.

Quantum Pirogov–Sinai theory acts, thus, as the link needed to pass from diagonalization—at the level of interactions—to phases. It is a powerful tool that can be used as a black box: Once the system is seen to be thermodynamic within its range of applicability there is nothing else to do;

the theory provides a flexible and complete description of the resulting phases. We know of no other comparably general and versatile approach to the study of quantum statistical mechanical phase diagrams. We see the methodological difference between quantum mechanics and quantum statistical mechanics. In the former, the ultimate goal is to diagonalize, *exactly*, the Hamiltonian of some system. In the latter, an exact diagonalization is impossible. The goal is then to do the *minimal* perturbative diagonalization needed to bring the system within the reach of some theory enabling us to determine the phase diagram, like our Pirogov–Sinai approach. Once such a theory takes over, we are done: All the required information is at our disposal; any further diagonalization is a waste of time.

4.2. Summary and hypotheses

4.2.1. Scope of the Theory. Quantum Pirogov–Sinai theory applies to interactions of the form (2.18), that is,

$$\Phi = \Phi^{\text{cl}} + Q \quad (4.2)$$

where $\Phi^{\text{cl}} = \{\Phi_X^{\text{cl}}\}$ is a finite range classical interaction (classical in the sense of Section 2.2), and $Q = \{Q_X\}$ is a possibly quantum interaction. The operators comprising both parts depend on a finite family of perturbation parameters $\lambda = \{\lambda_1, \dots, \lambda_k\}$. For our applications below, Φ^{cl} will be the leading part $\Phi_0^{(n)}$ of a transformed interaction of an appropriate order n . The theory has two consequences:

(PS1) *Stability of states:* Under suitable hypotheses, it determines the different periodic states of the full interaction, for small values of the parameters λ and small temperatures. Each of these states can be traced, in fact, to some ground state of Φ^{cl} , from which it differs in the addition of a diluted gas of thermal and quantum excitations. In such a case, the corresponding ground state of Φ^{cl} is said to be *stable* at the given temperature and values of λ .

(PS2) *Stability of phase diagrams:* It establishes (sufficient) conditions under which the zero-temperature phase diagram of the classical part remains “stable” under the addition of the quantum part, Q , and/or increasing temperature. That is, the manifolds where different phases coexist are, for small temperatures and quantum perturbations, smooth and small deformations of the corresponding coexistence manifolds of ground states of the classical part.

The theory requires two sets of hypotheses: (i) the classical leading part must have a finite ground-state degeneracy and satisfy the Peierls condition explained below, and (ii) the matrix elements of the quantum part must be sufficiently small.

4.2.2. Hypotheses on the Classical Part. Let us discuss the hypotheses on the classical part first. The finite degeneracy refers to the presence of only a finite number of *periodic* ground states for Φ^{cl} . In the present setting (m -potentials with minimal bond energies normalized to zero) these are configurations $\omega_1, \dots, \omega_p$ such that $\Phi_X^{\text{cl}}(\omega_i) = 0$ for all bonds X . The Peierls condition refers to the well known generalized Peierls contours.^(41, 40, 43) They are constructed by means of *sampling plaquettes*

$$W_x^{(a)} := \{y \in \mathbb{Z}^v : |y_i - x_i| \leq a, \text{ for } 1 \leq i \leq v\}, \quad \text{for } x \in \mathbb{Z}^v \quad (4.3)$$

The set of sampling plaquettes where a configuration ω does not coincide with any of the ground states ω_i is called the *defect set* of ω . The *contours* of ω are pairs $\gamma = (M, \omega_M)$, where M —the *support* of γ —is a maximally connected (with respect to intersections) component of the defect set. The radius a of the sampling plaquettes must be larger than the range of Φ^{cl} and the period of each of the ω_i , so that, knowing the set of contours, one can univocally reconstruct the configuration ω . In particular, when Φ^{cl} is a transformed interactions $\Phi_0^{(n)}$, a must be larger than the radius R of the plaquettes used to define protection zones (Section 2.2).

For models whose interactions and excitations are determined by nearest-neighbor conditions, like the Ising model, one can use the “thin” Peierls contours^(39, 13, 18) traced with segments midway between pairs of adjacent sites. But in more general cases one must resort to definitions as above to ensure a one-to-one correspondence between configurations and families of contours. The energy of a configuration is, in the present setting, the sum of energies, $E(\gamma)$, of contours γ . Here, $E(\gamma)$ is the energy of the configuration having γ as its only contour. A model satisfies the *Peierls condition* if each contour has an energy proportional to the cardinality of its support, $s(\gamma)$. That is,

$$E(\gamma) > \kappa s(\gamma) \quad (4.4)$$

for some $\kappa > 0$ called the *Peierls constant*.

In this paper, we consider a more detailed Peierls condition based on the distinction of two levels of excitations—low- and high-lying—of the classical part. The distinction is made through a suitably defined family of local projections P_Y^0 . With respect to this family, a configuration ω exhibits

a *high-lying excitation* in Y if $P_Y^0 \omega \neq \omega$. For the applications of this paper, these projections are exactly those defined in Section 2.2, because the low-lying excitations of $\Phi^{\text{cl}} = \Phi_0^{(n)}$ are among the local ground states of the original Φ_0 . The *high-energy defect set* of a configuration ω is the union of the plaquettes $W_x^{(a)}$ where it exhibits a high-lying excitation. A system satisfies a *two-level Peierls condition* if for each contour γ we have

$$E(\gamma) > \kappa s(\gamma) + Ds(\gamma^{\text{high}}) \quad (4.5)$$

where γ^{high} is the part of the high-energy defect set contained in γ . This condition means, in particular, that high-energy excitations lead to an additive *excess energy* measured by $D > 0$.

Given that Φ^{cl} is allowed to depend on the perturbation parameters λ , such a dependence is also expected for the Peierls constants κ and D .

4.2.3. Hypotheses on the Quantum Part. First, we decompose the operators of the quantum interaction, $Q = \{Q_X\}$, into “low \rightarrow low” ($\ell\ell$), “low \rightarrow high” (ℓh), “high \rightarrow low” ($h\ell$) and “high \rightarrow high” (hh) components:

$$\begin{aligned} Q_X^{\ell\ell} &:= P_X^0 Q_X P_X^0 \\ Q_X^{\ell h} &:= (\mathbf{1}_X - P_X^0) Q_X P_X^0 \\ Q_X^{h\ell} &:= P_X^0 Q_X (\mathbf{1}_X - P_X^0) \\ Q_X^{hh} &:= (\mathbf{1}_X - P_X^0) Q_X (\mathbf{1}_X - P_X^0) \end{aligned} \quad (4.6)$$

The conditions on the quantum part are that there exist sufficiently small numbers $\varepsilon_{\alpha\gamma}$ and δ such that, for $\alpha, \gamma = \ell, h$

$$\|Q_X^{\alpha\gamma}\| \leq \varepsilon_{\alpha\gamma} \delta^{s(X)} \quad (4.7)$$

The region of validity of the two-level quantum Pirogov theory depends on the parameter

$$\eta := \max \left(\frac{\varepsilon_{\ell\ell} \delta}{\kappa}, \delta \sqrt{\frac{\varepsilon_{h\ell} \varepsilon_{\ell h}}{\kappa(\kappa + D)}}, \frac{\varepsilon_{hh} \delta}{\kappa + D}, \frac{\varepsilon_{\ell h} \delta}{\kappa + D}, \frac{\varepsilon_{h\ell} \delta}{\kappa + D} \right) \quad (4.8)$$

Quantum Pirogov–Sinai theory converges provided η is sufficiently small.

The original (one-level) quantum Pirogov–Sinai theory discussed in refs. 11 and 5 corresponds to taking $D = \varepsilon_{h\ell} = \varepsilon_{\ell h} = \varepsilon_{hh} = 0$.

Interactions obtained as a result of the partial block-diagonalization procedure of Section 2, contain terms proportional to powers of λ/D ;

(λ measures the strength of the quantum perturbation, and D is proportional to a typical energy-denominator). Condition (4.7) thus imposes the bound

$$\max\left(\lambda, \frac{\lambda}{D}\right) < \delta \quad (4.9)$$

where δ is as in (4.7); (δ must be chosen small enough for the perturbation expansions to converge). The size of the $h\ell$ -matrix elements of the quantum perturbation, $\{Q_X \equiv Q_X^{(n)}(\lambda)\}$, in the Hamiltonian $H_A^{(n)}(\lambda)$ is estimated by

$$\|Q_X^{h\ell}\| \sim \|Q_X^{\ell h}\| \sim \frac{\lambda^{n+1}}{D^n} \delta^{s(X)-n-1} \quad (4.10)$$

Comparing (4.10) to (4.7) we find that

$$\varepsilon_{h\ell} = \varepsilon_{\ell h} = O\left(\frac{\lambda^{n+1}}{D^n \delta^{n+1}}\right) \quad (4.11)$$

As the “high \rightarrow high” part of the original interaction survives unaltered,

$$\varepsilon_{hh} = O\left(\frac{\lambda}{\delta}\right) \quad (4.12)$$

4.3. Stability of Phases

4.3.1. The Basic Criterion. Our criterion for the stability of phases is based on the use of cluster-expansion technology to construct some objects f'_1, \dots, f'_k —where f'_i is associated to the ground state ω_i of Φ^{cl} —called *truncated free energy densities*. They are defined provided that

$$\varepsilon := \max(e^{-\beta O(\kappa)}, \eta) < \varepsilon_0 \quad (4.13)$$

for some (small) constant ε_0 that depends on parameters like the range of Φ^{cl} , dimensionality of the lattice, size of the sampling plaquette, and dimension of the on-site Hilbert space. Within the convergence region, the truncated free energies are analytic functions of β and of any parameter on which the interaction has an analytic dependence. They determine the stability of phases in the following way.

Stability Criterion. Assume that λ is such that $\Phi^{\text{cl}}(\lambda)$ has a finitely degenerate ground state and satisfies the Peierls condition (4.5), and assume that $Q(\lambda)$ satisfies hypotheses (4.7). Then if, for some values of β and λ within the region (4.13),

$$\text{Re } f'_p(\underline{\mu}) = \min_{1 \leq q \leq k} \text{Re } f'_q(\underline{\mu}) \quad (4.14)$$

for some p with $1 \leq p \leq k$, the following holds:

- (i) $f'_p(\underline{\mu})$ coincides with the true free-energy density of the system;
- (ii) the infinite-volume limit

$$\lim_{A \nearrow \mathbb{Z}^d} \frac{\text{tr}_A^{\omega_p} \mathbf{A} e^{-\beta \mathbf{H}_A^{\omega_p}}}{\text{tr}_A^{\omega_p} e^{-\beta \mathbf{H}_A^{\omega_p}}} =: \langle \mathbf{A} \rangle_{\beta \lambda}^{\omega_p} \quad (4.15)$$

exists for any local operator \mathbf{A} ;

- (iii)

$$|\langle \mathbf{A} \rangle_{\beta \lambda}^{\omega_p} - \langle \omega_p | \mathbf{A} | \omega_p \rangle| \leq \|\mathbf{A}\| |X| O(\varepsilon) \quad (4.16)$$

for any operator $\mathbf{A} \in \mathcal{A}_X$, (X is a finite subset of the lattice).

The notation $H_A^{\omega_p}$ stands for the Hamiltonian with “external condition” ω_p , that is, the sum of all Φ_X with $X \cap A \neq \emptyset$, but allowing only matrix elements between vectors that coincide with ω_p outside A . The symbol $\text{tr}_A^{\omega_p}$ indicates a trace over the space of such vectors.

Note that, in (4.15), $H_A^{\omega_p}$ is the “effective” Hamiltonian, rather than the original Hamiltonian defining the model. The effective Hamiltonian and the original one are unitarily equivalent, the unitary conjugation being given by an operator $U_A^{(n)}(\lambda)$ as in (2.79), (2.82), (2.83). In order to select a stable phase, we impose boundary conditions ω_p outside boxes A on the *effective Hamiltonians* rather than the original Hamiltonians. One could reconstruct “boundary conditions” for the original Hamiltonians corresponding to the boundary conditions that we impose on the effective Hamiltonians. (Typically, “boundary conditions” for the original Hamiltonian will constrain configurations not only outside A but also inside A but near ∂A . We shall not attempt to provide details concerning the map from boundary conditions for the original Hamiltonians to boundary conditions for the effective Hamiltonians. Boundary conditions do *not* have an operational meaning here (corresponding, e.g., to certain experimental conditions), but are *mathematical devices to select stable phases* that should be chosen in as convenient a way as possible. In fact, this is the

conventional role of boundary conditions in statistical physics. When we describe a magnetic material in terms of a quantum Heisenberg model we are working with an *effective Hamiltonian*; (there are no explicit exchange interactions present in the fundamental Schrödinger Hamiltonian!). But we do not hesitate to impose boundary conditions directly on the Heisenberg Hamiltonian, rather than on the fundamental Schrödinger Hamiltonian of the material, in order to select stable pure phases (e.g., the direction of spontaneous magnetization).

We shall say that there is a *stable* ω_p -phase whenever (4.14) is satisfied.

We shall not enter here into the technicalities of the actual proof of this criterion, which can be found in ref. 11. Instead, we present some general comments on the basic construction.

The above criterion is proven by resorting to a low-temperature expansion obtained by iteration of Duhamel's formula for the exponential of the sum of non-commuting matrices. This adds an extra continuous variable ranging from 0 to β . There is one such expansion for each ground state of Φ^{cl} , involving a "sum" of terms labelled by the sites of the lattice ("spatial variables") and the continuous "inverse temperature" or "time" variable. Every term can be labelled by a piecewise cylindrical surface contained in $\mathbb{Z}^d \times [0, \beta]$, which can be decomposed into connected components called *quantum contours*. Outside the surface, the space is filled with the corresponding ground state of Φ^{cl} , and the contours are transition regions whose interiors are occupied by different ground states of Φ^{cl} . The contours have spatial sections formed by the usual classical contours described above, which grow cylindrically in the "time" direction until there is a sudden change of section due to the action of a quantum bond. The hypotheses on the quantum part ensure that the weight of this contour decays exponentially with its area: The exponential cost of each "vertical" cylindrical piece is given by the Peierls condition (4.5), while each "horizontal" change of section is penalized by a term (4.7) according to the type of transition involved. Each contour has a finite number of section changes.

We must distinguish between "short" and "long" contours. The long contours traverse the whole "time" axis from zero to β . Therefore, their cost is at least $\exp(-\text{const } \beta)$, and they disappear in the limit $\beta \rightarrow \infty$. In particular, a purely classical system would have *only* contours of this type which, in fact, would be straight cylinders with no section changes. "Short" contours appear and/or disappear at intermediate values of the continuous integration variable. Thus they involve some changes of sections, and their cost is proportional to δ . Such contours survive the limit $\beta \rightarrow \infty$ and contribute to the quantum ground state of the full interaction Φ .

We see that, in this approach, thermal and quantum effects are put on a similar footing. They are both sources of entropy associated to different contour geometries. A low-temperature equilibrium state can be visualized as a “sea” configured of the corresponding ground state of Φ^{cl} plus the fluctuations represented by contours. In particular, the short contours can be interpreted as “ground state fluctuations.” At low temperatures and small values of δ , these fluctuations are dilute, because their large energy cost overwhelms the “entropy gain.” Thus expectations in such a state differ little from expectations in the associated ground state of Φ^{cl} .

4.3.2. Stability and Symmetries. Two types of symmetries can be distinguished. First, there are symmetries that leave each term of the interaction (or of an equivalent form of it) invariant. Such a symmetry is associated, for each finite volume Λ , to a unitary operator S_Λ such that

$$S_\Lambda H_\Lambda^{\omega_p} S_\Lambda^{-1} = H_\Lambda^{S\omega_p} \quad (4.17)$$

[The vector $S\omega_p$ is easy to visualize at the level of classical configurations. In a quantum statistical mechanical formalism, it is defined, for instance, via limits of $S_\Lambda^{-1}\omega_p$.] Examples of these symmetries are the spin-flip symmetry of Ising models in zero field, or the particle-hole symmetry of the Hubbard model at half filling.

On the other hand, there are symmetries associated to operations on the lattice, like translations and rotations. They map each term of the interaction into a different term, but leave the whole interaction invariant. Each such symmetry is defined by a bijection $T: \mathbb{Z}^d \rightarrow \mathbb{Z}^d$ that yields natural bijective maps between configurations— $(T\omega)_x = \omega_{T^{-1}x}$ —and between local operators— $(T\Phi)_x = \Phi_{T^{-1}x}$ (for notational simplicity we denote the different transformations with the same symbol). The latter map does not leave Hamiltonians invariant, but connects Hamiltonians corresponding to translated volumes:

$$TH_\Lambda^{\sigma_p} T^{-1} = H_{T^{-1}\Lambda}^{T\sigma_p} \quad (4.18)$$

In general, a symmetry, R , can be a composition, ST , of symmetries of the previous two types.

The criterion of stability of phases presented above respects symmetries. Indeed, we say that a symmetry R *connects* a family of configurations $\{\omega_1, \dots, \omega_\ell\}$ if

$$R^i \omega_1 = \omega_{i+1} \quad \text{for } 1 \leq i \leq \ell - 1 \quad (4.19)$$

Then, under the hypotheses of the preceding subsection, we have:

$$\begin{aligned} & \text{Ground states of } \Phi^{\text{cl}} \text{ connected by a symmetry} \\ & \text{of } \Phi \text{ are either all stable or all unstable} \end{aligned} \quad (4.20)$$

We briefly sketch a proof of this fact, as it is not explicitly given in ref. 11 or in ref. 12. The key object to look at is the partition function $\Xi_p(V)$ for piecewise cylindrical, bounded regions, V , of $\mathbb{Z}^d \times [0, \beta]$. This object is defined, through the contour expansion, as the sum of all allowed contour configurations inside V compatible with the boundary condition ω_p . For regions V of the form $A \times [0, \beta]$, with A a finite region of \mathbb{Z}^d , one has

$$\Xi_p(A) = \text{tr}_A^{\omega_p} e^{-\beta \mathbf{H}_A^{\omega_p}} \quad (4.21)$$

Looking carefully into the definition of $\Xi(V)$, it is not hard to conclude that its behavior with respect to symmetries is similar to that of (4.21). Namely, if S a symmetry of the first type,

$$\Xi_{S\omega_p}(V) = \Xi_{\omega_p}(V) \quad (4.22)$$

and, if T is a symmetry of the second type

$$\Xi_{T\omega_p}(V) = \Xi_{\omega_p}(T^{-1}V) \quad (4.23)$$

Here $T^{-1}V$ refers to the space-time region V transformed by the map T^{-1} .

These partition functions are involved in the following characterization of stability: A ground state ω_p of Φ^{cl} is stable in the region (4.13) if, and only if, there exists some constant C such that

$$\left| \frac{\Xi_{\omega_j}(V)}{\Xi_{\omega_p}(V)} \right| \leq \exp(C |\partial V|) \quad (4.24)$$

for every bounded region $V \subset \mathbb{Z}^d \times [0, \beta]$ and $1 \leq j \leq k$. Here $|\partial V|$ indicates the area of the external boundary of V .

The criterion (4.20) is now easy to verify: Assume that some ground states $\omega_1, \dots, \omega_\ell$ are connected by a symmetry. If the symmetry is of the first type, then by (4.22)

$$\Xi_1(V) = \dots = \Xi_\ell(V) \quad (4.25)$$

for all piecewise cylindrical $V \subset \mathbb{Z}^d \times [0, \beta]$. Hence (4.24) is either verified by all $p = 1, \dots, \ell$ or by none.

Consider then a symmetry of the second type, and assume, for concreteness, that ω_ℓ is stable. Then (4.24) is verified for $p = \ell$ and all j , in particular for $j = q$ where $\omega_q = T^{-(\ell-q)}\omega_\ell$ ($1 \leq q \leq \ell$) [see (4.19)]. But then, from (4.23) we have

$$\left| \frac{\Xi_{\omega_\ell}(V)}{\Xi_{\omega_q}(V)} \right| = \left| \frac{\Xi_{\omega_{\ell-q}}(T^{-(\ell-q)}V)}{\Xi_{\omega_\ell}(T^{-(\ell-q)}V)} \right| \leq \exp(C |\partial V|) \quad (4.26)$$

The last inequality follows from the assumed stability of ω_ℓ and the fact that $|\partial(TV)| = |\partial V|$. Therefore, for any $1 \leq q \leq \ell$, and any $1 \leq j \leq k$,

$$\left| \frac{\Xi_{\omega_j}(V)}{\Xi_{\omega_q}(V)} \right| = \left| \frac{\Xi_{\omega_j}(V)}{\Xi_{\omega_\ell}(V)} \right| \left| \frac{\Xi_{\omega_\ell}(V)}{\Xi_{\omega_q}(V)} \right| \leq \exp(2C |\partial V|) \quad (4.27)$$

where the inequality follows from the stability of ω_ℓ [Eq. (4.24)] and from (4.26). We conclude that all the ground states $\omega_1, \dots, \omega_\ell$ are stable (with an exponential constant $2C$).

4.4. Stability of Phase Diagrams

More generally, one studies families of interactions Φ_μ parametrized by a finite set of parameters $\mu = \{\mu_1, \dots, \mu_s\}$ —typically fields or chemical potentials—and one is interested in determining the corresponding *phase diagram*, that is, in obtaining a catalogue of the different phases present for different values of μ . If for the values of μ under consideration the system satisfies the hypotheses described above, one can apply quantum Pirogov–Sinai theory and determine the phase diagram on the basis of condition (4.14), now involving μ -dependent truncated free energies f'_p . The cluster expansion tells us that the difference between these truncated free energies and the corresponding energy densities is of the order of the parameter $\varepsilon_{\beta\lambda}$ introduced in (4.13). Therefore, given the smoothness properties of f'_p , one would expect that the phase diagram, for β and λ in the region (4.13), differs little from the phase diagram of Φ^{cl} at zero temperature.

This can, indeed, be proven, under some minor additional hypotheses: Chiefly, (i) bounds similar to (4.7) but involving the partial derivatives $\partial Q_{\mu X} / \partial \mu_i$, and (ii) a hypothesis of *regularity* of the phase diagram of Φ_μ^{cl} . The latter roughly means that the parameters μ completely break degeneracies among the ground states, so the Gibbs phase rule is satisfied. The detailed hypotheses can be found in [12, Section 5.2]. The conclusion is:

If the hypotheses sketched above are satisfied for an open region \mathcal{O} of the space of parameters μ , then the phase diagram for β and λ in a region

of the form (4.13) is regular and is a smooth deformation of the zero-temperature phase diagram of Φ_μ^{cl} in \mathcal{O} . The displacement of the different coexistence manifolds is of the order of $\varepsilon_{\beta\lambda}$.

5. PHASE DIAGRAM FOR THE FALICOV–KIMBALL REGIME

We now apply the phase-diagram technology described in the previous section to asymmetric Hubbard models, whose perturbation expansion has been discussed in Section 3. Let us denote

$$t = \sup_{[x, y]} |t_-^{[x, y]}| \quad (5.1)$$

$$t_+ = \sup_{[x, y]} |t_+^{[x, y]}| \quad (5.2)$$

(with a slight abuse of notation). Let us see how further features of the phase diagram appear as we consider higher orders in the perturbation expansion.

5.1. Phase Diagram to Order t^0

To this order, the classical leading interaction correspond to a (formal) Hamiltonian

$$H^{\text{cl}(0)} = U \sum_x n_{x+} n_{x-} - \mu_+ \sum_x n_{x+} - \mu_- \sum_x n_{x-} \quad (5.3)$$

We see from Fig. 1 that it trivially satisfies the hypotheses of Section 4.2.2—in fact for the one-level theory—as long as one avoids the lines where the different regions with a unique ground state intersect. In the latter we loose the required finite degeneracy. The conclusion is, therefore, that different ground states remain stable for chemical potentials in the open regions of uniqueness. The range (4.13) shrinks to zero as we approach a coexistence manifold, because so do the different Peierls constant (which are of the order of the energy of the lowest excitation). This phase stability remains true upon the addition of electron hopping or *any* quantum perturbation which is translation-invariant and satisfies $\eta \leq \varepsilon_0$ (for instance small ion-hopping).

5.2. Phase Diagram to Order t^2/U

To this order we can exhibit more features of the phase diagram within the shaded region in Fig. 2. The transformed interaction was

obtained in Section 3.4 [Formula (3.30)]. It has a leading classical part

$$H^{\text{cl}(1)} = U \sum_x n_{x+} n_{x-} + \frac{2}{U} \sum_{\langle xy \rangle} |t_{-}^{[x,y]}| \left(S_x^3 S_y^3 - \frac{P_{\{x,y\}}^0}{4} \right) - h \sum_x S_x^3 \quad (5.4)$$

whose periodic ground-state configurations are given in Fig. 3. This interaction satisfies a two-level Peierls condition. The low-lying excitations have one particle per site and involve a Peierls constant

$$\kappa \sim 4t^2/U \pm h + O(t^4/U^3) \quad (5.5)$$

The excess energy for configurations in the non-singly occupied band gives an extra Peierls rate

$$D = \max(U - \mu_0, \mu_0) = O(U) \quad (5.6)$$

(μ_0 defines the boundaries of the shaded region in Fig. 2; for concreteness we are considering $\mu_0 \sim U$). We see that the leading part (5.4) satisfies the hypotheses required for the classical part in Section 4.2.2 as long as

$$4t^2/U \pm h + O(t^4/U^3) > 0 \quad (5.7)$$

that is, except within bands of width $O(t^4/U^3)$ centered at the lines $h = \pm 4t^2/U$. Moreover, the summability of the transformed interaction is guaranteed only if $D \gg \kappa$. This condition determines the limits of the shaded region in Fig. 2.

The “low \rightarrow low” transitions must include at least one ionic jump, hence a factor t_+ . Therefore [see e.g., the quantum correction in (3.30)],

$$\varepsilon_{\ell\ell} = O\left(\frac{t_+}{t} \cdot \frac{t^2}{U\delta}\right) \quad (5.8)$$

where δ has been chosen sufficiently small to guarantee the convergence of the partially diagonalized interaction. From this, (4.11) (with $n = 1$) and (4.12) we see that the quantum perturbation satisfies hypotheses (4.13) if

$$\frac{t_+}{t}, \frac{t}{U} < \tilde{\varepsilon}_0 \quad (5.9)$$

where $\tilde{\varepsilon}_0$ is a small number that shrinks to zero when κ tends to zero (and at the boundaries of the shaded region in Fig. 2).

We conclude that quantum Pirogov–Sinai theory [together with the symmetry criterion (4.20)] proves that for *nonzero* but small values of t ,

the phase diagram of the model is as in Fig. 4. The ground states correspond to the configurations shown in the figure plus quantum fluctuations (= short space-time contours). Furthermore, they remain stable for small temperatures (long contours appear sparingly) and small values of t_+ (new contours appear, rarely, involving the new type of quantum transitions). This picture is valid outside an excluded $O(t^4/U^3)$ -vicinity of the lines $h = \pm 2t^2/U$ where the Peierls constant κ cannot be guaranteed to be positive, and inside the shaded region of Fig. 2 where $\kappa \ll D$. This stability persists under the addition of arbitrary quantum perturbations satisfying (4.7) that do not break translation invariance.

5.3. Phase Diagram up to Order t^4/U^3

In order to analyze in more detail the excluded regions of widths $O(t^4/U^3)$, we need to consider the next order of perturbation theory. For the direction-independent case ($t_-^b \equiv t$), the leading classical interaction, to this order, is given by the terms in Table 2. At this point, the hardest part of the analysis is, by far, the determination of the ground states of this complicated classical part. Fortunately, this has been done before, see refs. 31 and 23: the ground states correspond to the configurations depicted in Fig. 5. We see that the classical part, to fourth order, satisfies the hypotheses required by Pirogov–Sinai theory, except in the vicinity of four lines of infinite degeneracy. In regions at a distance $O(t^6/U^5)$ from these lines, the Peierls constant κ is of order t^4/U^3 . The gap D is still given by (5.6).

Moreover, the quantum part has coefficients $\varepsilon_{h\ell}$ and $\varepsilon_{\ell h}$ given by (4.11) with $n = 2$, and ε_{hh} given by (4.12), while

$$\varepsilon_{\ell\ell} = O\left(\frac{t_+}{t} \cdot \frac{t^4}{U^3 \delta^4}\right) \quad (5.10)$$

[see e.g., the quantum corrections in Table 1].

As a consequence, the stability criterion of Section 4.3.1 is applicable, for large β and t satisfying (5.9) with a smaller $\tilde{\varepsilon}_0$. Together with the symmetry considerations (4.20), this implies the stability of the ground states of Fig. 5—except at the excluded bands of width $O(t^6/U^5)$ around the coexistence lines—under the addition of temperature, ionic hopping [within the limits imposed by (5.9)], and any other translation- and rotation-invariant quantum perturbation satisfying (4.13). The phase diagram of Fig. 5 is thus obtained.

A similar analysis can be performed for cases in which the hopping depends on the direction. In particular, in the presence of magnetic flux,

i.e., if $t_{-yx}^{[yx]} = t \exp(i\theta_{yx})$ with $\theta_{yx} \in (0, 2\pi)$, our block-diagonalization procedure yields, to order t^4/U^3 , an effective classical interaction with terms given in [23, Formula (3.11)]. As shown in this reference, the phase diagram for the interaction with flux involves the same ground states as in the flux-less case, but with deformed manifolds of infinite degeneracy. The Pirogov–Sinai approach proves the stability of these ground states, under quantum and thermal perturbations, except in excluded regions of width t^6/U^5 around the lines of infinite degeneracy.

6. PERTURBATION EXPANSION FOR THE 3-BAND HUBBARD MODEL

In all the models considered in the previous section, the Coulomb interactions between the particles were strictly on-site. In this section we apply our perturbation method to the 3-band Hubbard model, as an example of how to proceed when the leading interaction has nonzero range.

6.1. The Original Interaction

The Hamiltonian $H_{0,d}$ in (1.2) is of unit range, since it consists of both on-site and nearest neighbor interactions. This necessitates the use of “protection zones” [see Section 2.2] for the proper treatment of the local character of the operators that arise in our perturbation expansion. We define R -plaquettes, W_x , through (2.23) with $R=1$, and sets B_x through (2.24). In particular, for $X := \langle xy \rangle$, $x \in A$, $y \in B$, $|x - y| = 1$, B_x is given by the set of sites shown in Fig. 8 (or a rotation and/or reflection of it).

It consists of two copper sites and four oxygen sites. We restrict our attention to parameter values in the following ranges:

$$U_d > \varepsilon_d; \quad \Delta > 0; \quad U_d \gg U_p > U_{pd} > 0; \quad U_d \gg \Delta; \quad t_{pd} > 0; \quad U_d \gg t_{pd} \quad (6.1)$$

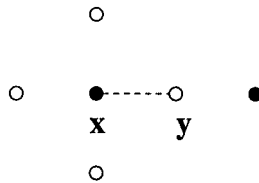


Fig. 8. Set B_x formed by the bond $\langle xy \rangle$ and its protection zone for the 3-band Hubbard model.

and normalize the ground state energy of H_{0A} to zero. The unperturbed Hamiltonian is given in terms of an interaction $\Phi_0 = \{\Phi_{0Y}\}$, nonzero, if $Y = \langle xy \rangle$ denotes a pair of nearest neighbor sites such that $x \in A$ and $y \in B$. The interaction Φ_{0X} is defined as follows.

$$\Phi_{0Y} = \begin{cases} U_d n_{x+}^d n_{x-}^d + \varepsilon_d (n_x^d - 1) & \text{if } Y = \{x\}, x \in A \\ U_p n_{y+}^p n_{y-}^p + \varepsilon_p n_y^p & \text{if } Y = \{y\}, y \in B \\ U_{pd} n_x^d n_y^p & \text{if } Y = \langle xy \rangle, x \in A, y \in B \end{cases} \quad (6.2)$$

For parameter values satisfying (6.1), the energy of a configuration on Y , with respect to the interaction Φ_{0Y} , is minimum (and equal to zero) when there is a single hole at x and none at y . Hence in a ground state configuration of H_{0A} , each oxygen site is empty while each copper site is singly occupied by a hole, the total number of holes in A being equal to the total number of copper sites, $|A|$. However, the ground state of H_{0A} has a $2^{|A|}$ -fold spin degeneracy.

The interaction corresponding to the 3-band Hubbard Hamiltonian H_A (1.2), with the normalization introduced above, is given by $\Phi = \{\Phi_Y\}$ where

$$\Phi_Y = \Phi_{0Y} + Q_Y \quad (6.3)$$

and $Q_Y = 0$ unless Y is a pair of nearest-neighbor sites, in which case

$$Q_{\{xy\}} = t_{pd} [p_{y\sigma}^\dagger d_{x\sigma} + d_{y\sigma}^\dagger p_{x\sigma}] \quad (6.4)$$

We define suitable projection operators on the Hilbert space \mathcal{H}_A as in Section 2.2. Let $P_{B_x}^0$ denote an operator which projects onto (local) ground states of the interaction Φ_0 . The projection operators $P_{B_x}^1$ and $P_{B_x}^2$ are defined by (2.25) and (2.26) of Section 2.2. Using the resulting partition of unity

$$\mathbf{1} = P_{B_x}^0 + P_{B_x}^1 + P_{B_x}^2 \quad (6.5)$$

we can decompose the perturbation interaction Q_X of (6.4) as in (2.37). It is clear from the structure of the lattice [Fig. 6] and the definition (6.4) of Q_X that $Q_{B_y}^{00} = 0$. Hence

$$Q_X = Q_{B_x}^{01} + Q_{B_x}^R \quad (6.6)$$

where $Q_{B_x}^{01}$ and $Q_{B_x}^R$ —defined in (2.39) and (2.40)—are linear in the hopping amplitude t_{pd} . Also, due to our choice of ground-state energy normalization,

$$\Phi_{0B_x}^{00} = 0 \quad (6.7)$$

6.2. First-Order Perturbation for the 3-Band Hubbard Model

As explained in Section 2, we first search for a unitary transformation $U^{(1)}(t_{pd}) = \exp(t_{pd}S_1)$ with

$$S_1 := \sum_X S_{1B_X} \quad (6.8)$$

which eliminates the first-order off-diagonal terms $Q_{B_X}^{01}$ of the perturbation interaction Q . From (2.50) we have that

$$S_{1B_X} = P_{B_X}^0 \frac{Q_{B_X}}{E_0 - E_1} P_{B_X}^1 + P_{B_X}^1 \frac{Q_{B_X}}{E_1 - E_0} P_{B_X}^0 \quad (6.9)$$

where

$$E_0 = 0 \quad \text{and} \quad E_1 = U_{pd} + \Delta \quad (6.10)$$

with

$$\Delta := \varepsilon_p - \varepsilon_d \quad (6.11)$$

Hence

$$S_{1B_X} = \frac{1}{U_{pd} + \Delta} \{ P_{B_X}^1 Q_{B_X} P_{B_X}^0 - P_{B_X}^0 Q_{B_X} P_{B_X}^1 \} \quad (6.12)$$

for $X \equiv \langle xy \rangle$, $x \in A$ and $y \in B$. A straightforward calculation along the lines sketched in Section 2.3 shows that the transformed classical interaction has nonzero terms only for nearest-neighbor pairs X . These terms are [recall (6.7)]:

$$\begin{aligned} \Phi_{0B_X}^{(1)} &= \frac{1}{2} P_{B_X}^0 \text{ad } S_{1B_X} (Q_{B_X}^{01}) P_{B_X}^0 \\ &= -\frac{t_{pd}^2}{(U_{pd} + \Delta)} P_{B_X}^0 \left[\sum_{\sigma=+, -} d_{x\sigma}^\dagger p_{y\sigma} p_{y\sigma}^\dagger d_{x\sigma} \right] P_{B_X}^0 \\ &= -\frac{t_{pd}^2}{(U_{pd} + \Delta)} P_{B_X}^0 \left(\sum_{\sigma=+, -} n_{x\sigma}^d (1 - n_{y\sigma}^p) \right) P_{B_X}^0 \\ &= -\frac{t_{pd}^2}{(U_{pd} + \Delta)} P_{B_X}^0 \end{aligned} \quad (6.13)$$

In the last line we used the identity

$$P_{B_X}^0 \left(\sum_{\sigma=+,-} n_{x\sigma}^d (1 - n_{y\sigma}^p) \right) P_{B_X}^0 = P_{B_X}^0 \left(\sum_{\sigma=+,-} n_{x\sigma}^d \right) P_{B_X}^0 = 1 \quad (6.14)$$

We conclude that, to this order, the change in the classical interaction amounts to an irrelevant shift in the (local) ground-state energy that does not introduce any new effect. In particular, it fails to reduce the spin degeneracy. We need to go to the next order of our perturbation scheme to find non-trivial contributions.

6.3. Second-Order Perturbation for the 3-Band Hubbard Model

From Section 2.4 we obtain that, in second-order perturbation theory, the leading classical part, $\Phi_0^{(2)} = [\Psi_0^{(2)}]^{00}$, is of the form

$$\Phi_0^{(2)} = \Phi_0^{(1)} + \varphi_0^{(2)} \quad (6.15)$$

where the nonzero terms of the latter are

$$\varphi_{0B_X}^{(2)} = \frac{1}{8} P_{B_X}^0 [\text{ad } S_{1B_X} (\text{ad } S_{1B_X} (\text{ad } S_{1B_X} (Q_{B_X}^{01})))] P_{B_X}^0 \quad (6.16)$$

for X a nearest-neighbor pair, and

$$\begin{aligned} \varphi_{0B_Y}^{(2)} &= \frac{1}{8} \sum_{C_6} P_{B_Y}^0 [\text{ad } S_{1B_{X_4}} (\text{ad } S_{1B_{X_3}} (\text{ad } S_{1B_{X_2}} (Q_{B_{X_1}}^{01})))] P_{B_Y}^0 \\ &\quad + \frac{1}{2} \sum_{C_4} P_Y^0 [\text{ad } S_{2(B_{X_4} \cup B_{X_3})} (V_{2(B_{X_1} \cup B_{X_2})}^{01})] P_Y^0 \end{aligned} \quad (6.17)$$

for $Y = X \cup X'$, where $X = \langle xy \rangle$, $X' = \langle yz \rangle$ are pairs of nearest neighbor sites with $x, z \in A$ and $y \in B$. See the notes at the bottom of Table 1 for the definition of C_6 and C_4 .

The one-bond contribution (6.16) is again an uninteresting energy shift:

$$\varphi_{0B_{\{x,y\}}}^{(2)} = \frac{t_{pd}^4}{(U_{pd} + \Delta)^3} P_{B_{\{x,y\}}}^0 \quad (6.18)$$

The two-bond contribution (6.17) can be cast in a more familiar-looking form by making use of spin operators at copper sites, [see (3.19)]:

$$\mathbf{S}_x := \sum_{s, s' = +, -} d_{xs}^\dagger \mathbf{S}_{ss'} d_{xs'} \quad (6.19)$$

One obtains

$$\varphi_{0\mathbf{B}_{\{x, y, z\}}}^{(2)} = \left[\frac{2t_{pd}^4}{(U_p d + \Delta)^3} \right] P_{\mathbf{B}_{\{x, y, z\}}}^0 + J_{\text{eff}} P_{\mathbf{B}_{\{x, y, z\}}}^0 \left(\mathbf{S}_x \cdot \mathbf{S}_z - \frac{1}{4} \right) P_{\mathbf{B}_{\{x, y, z\}}}^0 \quad (6.20)$$

with

$$J_{\text{eff}} := \frac{4t_{pd}^4}{(U_{pd} + \Delta)^2} \left[\frac{1}{U_d} + \frac{2}{2\Delta + U_p} \right] \quad (6.21)$$

From (6.15), (6.13), (6.18) and (6.20) we recover the known fact that the effective Hamiltonian for the 3-band Hubbard model in the low-energy sector, to order 4 in the hopping amplitude t_{pd} , is given by a $S=1/2$ antiferromagnetic Heisenberg model on the square lattice of copper sites. This is the same interaction obtained for the one-band Hubbard model to order t^2 [Table 2]. This observation justifies, in part, the use of the simpler one-band model in studies of magnetic properties of undoped cuprates. Our contribution is, once again, to be able to provide convergent estimates on remainder terms in the transformed interaction.

ACKNOWLEDGMENTS

We thank Daniel Ueltschi for informing us about his work with Roman Kotecký. We also thank Christian Borgs, Jennifer T. Chayes and Luc Rey-Bellet for their interest in our work. R. F. is grateful to the Institute de Physique Théorique, EPF-Lausanne, and the Institut für Theoretische Physik, ETH-Zürich, for hospitality during the completion of this work. He also wishes to acknowledge travel support by FAPESP (Grant 1998/3366-4). R.F. is a researcher of the National Research Council (CONICET), Argentina. This work was partially supported by CNPq (Grant 301625/95-6), FAPESP 95/0790-1 (Projeto Temático “Fenômenos críticos e processos evolutivos e sistemas em equilíbrio”) and FINEP (Núcleo de Excelência “Fenômenos críticos em probabilidade e processos estocásticos” PRONEX-177/96).

REFERENCES

1. C. Albanese, On the spectrum of the Heisenberg Hamiltonian, *J. Stat. Phys.* **55**:297–309 (1989).
2. C. Albanese, Unitary dressing transformations and exponential decay below threshold for quantum spin systems, Parts I and II, *Commun. Math. Phys.* **134**:1–27 (1990).
3. C. Albanese, Unitary dressing transformations and exponential decay below threshold for quantum spin systems, Parts III and IV, *Commun. Math. Phys.* **134**:237–272 (1990).
4. P. W. Anderson, New approach to the theory of superexchange interactions, *Phys. Rev.* **115**:2–13 (1959).
5. C. Borgs, R. Kotecký, and D. Ueltschi, Low temperature phase diagrams for quantum perturbations of classical spin systems, *Commun. Math. Phys.* **181**:409–46 (1996).
6. J. Bricmont and J. Slawny, First order phase transitions and perturbation theory, in *Statistical Mechanics and Field Theory: Mathematical Aspects (Proceedings, Groningen, 1985)*, T. C. Dorlas, N. M. Hugenholtz, and M. Winnink, eds. (Springer-Verlag, Berlin/Heidelberg/New York, 1986) (Lecture Notes in Physics, Vol. 257).
7. J. Bricmont and J. Slawny, Phase transitions in systems with a finite number of dominant ground states, *J. Stat. Phys.* **54**:89–161 (1989).
8. L. N. Bulaevskii, Quasihomopolar electron levels in crystals and molecules, *Zh. Eksp. Teor. Fiz.* **51**:230–40 (1966). [*Sov. Phys. JETP* **24**:154–60 (1967)].
9. K. A. Chao, J. Spalek, and A. M. Oleś, Kinetic exchange interaction in a narrow *S*-band, *J. Phys. C* **10**:L271–6 (1977).
10. K. A. Chao, J. Spalek, and A. M. Oleś, Canonical perturbation expansion of the Hubbard model, *Phys. Rev. B* **18**:3453–64 (1978).
11. N. Datta, R. Fernández, and J. Fröhlich, Low-temperature phase diagrams of quantum lattice systems. I. Stability for quantum perturbations of classical systems with finitely-many ground states, *J. Stat. Phys.* **84**:455–534 (1996).
12. N. Datta, R. Fernández, J. Fröhlich, and L. Rey-Bellet, Low-temperature phase diagrams of quantum lattice systems. II. Convergent perturbation expansions and stability in systems with infinite degeneracy, *Helv. Phys. Acta* **69**:752–820, 1996. Reprinted in *The Mathematical Side of the Coin. Essays in Mathematical Physics* (Birkhäuser, 1996).
13. R. L. Dobrushin, Existence of a phase transition in the two-dimensional and three-dimensional Ising models, *Soviet Phys. Doklady* **10**:111–113 (1965).
14. H. Eskes, A. M. Oleś, M. B. J. Meinders, and W. Stephan, Spectral properties of the Hubbard model, *Phys. Rev. B* **50**:17980–8002 (1994).
15. K. Friedrichs, *Perturbation of Spectra in Hilbert Space*, Am. Math. Soc. (Providence, R.I., 1965).
16. J. Fröhlich and L. Rey-Bellet, Low-temperature phase diagrams of quantum lattice systems. III. Examples. *Helv. Phys. Acta* **69**:821–849, 1996. Reprinted in *The Mathematical Side of the Coin. Essays in Mathematical Physics* (Birkhäuser, 1996).
17. J. Glimm, Boson fields with the: Φ^4 : interaction in three dimensions, *Commun. Math. Phys.* **10**:1–47 (1968).
18. R. B. Griffiths, Peierls' proof of spontaneous magnetization of a two-dimensional Ising ferromagnet, *Phys. Rev. A* **136**:437–439 (1964).
19. C. Gross, R. Joynt, and T. M. Rice, Antiferromagnetic correlations in almost-localized Fermi liquids, *Phys. Rev. B* **36**:381–93 (1987).
20. C. Gruber, J. Iwanski, J. Jędrzejewski, and P. Lemberger, Ground states of the spinless Falicov–Kimball model, *Phys. Rev. B* **41**:2198–209 (1990).
21. C. Gruber, J. Jędrzejewski, and P. Lemberger, Ground states of the spinless Falicov–Kimball model. II, *J. Statist. Phys.* **66**:913–38 (1992).

22. C. Gruber and N. Macris, The Falicov–Kimball model: A review of exact results and extensions, *Helv. Phys. Acta* **69**:850–907 (1996). Reprinted in *The Mathematical Side of the Coin. Essays in Mathematical Physics* (Birkhäuser, 1996).
23. C. Gruber, N. Macris, A. Messenger, and D. Ueltschi, Ground states and flux configurations of the two-dimensional Falicov–Kimball model, *J. Statist. Phys.* **86**:57–108 (1997).
24. C. Gruber and A. Sütő, Phase diagrams of lattice systems of residual entropy, *J. Stat. Phys.* **42**:113–142 (1988).
25. C. Gruber, D. Ueltschi and J. Jędrzejewski, Molecule formation and the Farey tree in the one-dimensional Falicov–Kimball model, *J. Stat. Phys.* **76**:125–157 (1994).
26. A. B. Harris and R. V. Lange, Single-particle excitations in narrow energy bands, *Phys. Rev.* **157**:295–314 (1967).
27. W. Holsztyński and J. Slawny, Peierls condition and the number of ground states, *Commun. Math. Phys.* **61**:177–190 (1978).
28. M. Hybertsen, M. Schlüter, and N. E. Christensen, Calculation of Coulomb-interaction parameters for La_2CuO_4 using a constrained-density-functional approach, *Phys. Rev. B* **39**:9028–41 (1989).
29. M. Hybertsen, E. B. Stechel, M. Schlüter, and D. R. Jennison, Renormalization from density functional theory to strong-coupling models for electronic states in Cu-O materials, *Phys. Res. B* **41**:11068–72 (1990).
30. T. Kato, *Perturbation Theory for Linear Operators* (Springer-Verlag, Berlin/Heidelberg/New York, 1966).
31. T. Kennedy, Some rigorous results on the ground states of the Falicov–Kimball model, *Rev. Math. Phys.* **6**:901–25 (1994).
32. T. Kennedy and E. H. Lieb, An itinerant electron model with crystalline or magnetic long range order, *Physica A* **138**:320–58 (1986).
33. D. J. Klein and W. A. Seitz, Perturbation expansion of the linear Hubbard model, *Phys. Rev. B* **8**:2236–47 (1973).
34. R. Kotecký, L. Laanait, A. Messenger, and S. Miracle-Solé, A spin-1 lattice model of microemulsions at low temperatures, *J. Phys. A* **26**:5285–93 (1993).
35. R. Kotecký and D. Ueltschi, Effective interactions due to quantum fluctuations. Preprint (1998), can be retrieved from http://www.ma.utexas.edu/mp_arc/, preprint 98-258.
36. J. L. Lebowitz and N. Macris, Long range order in the Falicov–Kimball model: Extension of Kennedy–Lieb theorem, *Rev. Math. Phys.* **6**:927–46 (1994).
37. A. H. MacDonald, S. M. Girvin, and D. Yoshioka, t/U expansion for the Hubbard model, *Phys. Rev. B* **37**:9753–6 (1988).
38. A. Messenger and S. Miracle-Solé, Low temperature states in the Falicov–Kimball model, *Rev. Math. Phys.* **8**:271–99 (1996).
39. R. Peierls, Ising’s model of ferromagnetism, *Proc. Cambridge Philos. Soc.* **32**:477–481 (1936).
40. S. A. Pirogov and Ya. G. Sinai, Phase diagrams of classical lattice systems, Continuation, *Theor. Math. Phys.* **26**:39–49 (1976). [Russian original: *Theor. Mat. Fiz.* **26**:61–76 (1976)].
41. S. A. Pirogov and Ya. G. Sinai, Phase diagrams of classical lattice systems. I, *Theor. Math. Phys.* **25**:1185–92 (1976). [Russian original: *Theor. Mat. Fiz.* **25**:358–69 (1975)].
42. M. Reed and B. Simon, *Methods of Modern Mathematical Physics IV: Analysis of Operators* (Academic Press, New York/London, 1978).
43. Ya. G. Sinai, *Theory of Phase Transitions: Rigorous Results* (Pergamon Press, Oxford/New York, 1982).
44. J. Slawny, Low temperature properties of classical lattice systems: phase transitions and phase diagrams, in *Phase Transitions and Critical Phenomena*, Vol. 11, C. Domb and J. L. Lebowitz, eds. (Academic Press, London/New York, 1985).

45. M. Takahashi, Half-filled Hubbard model at low temperatures, *J. Phys. C* **10**:1289–301 (1977).
46. H. Tasaki, The Hubbard model: Introduction and some rigorous results, *Markov Proc. Rel. Fields* **2**:183–208 (1996).
47. G. I. Watson and R. Lemanski, The ground-state phase diagram of the two-dimensional Falicov–Kimball model, *J. Phys. Condens. Matter* **7**:9521–42 (1994).